INFORMATION TO USERS

This material was produced from a microfilm copy of the original document. While the most advanced technological means to photograph and reproduce this document have been used, the quality is heavily dependent upon the quality of the original submitted.

The following explanation of techniques is provided to help you understand markings or patterns which may appear on this reproduction.

1. The sign or "target" for pages apparently lacking from the document photographed is "Missing Page(s)". If it was possible to obtain the missing page(s) or section, they are spliced into the film along with adjacent pages. This may have necessitated cutting thru an image and duplicating adjacent pages to insure you complete continuity.

2. When an image on the film is obliterated with a large round black mark, it is an indication that the photographer suspected that the copy may have moved during exposure and thus cause a blurred image. You will find a good image of the page in the adjacent frame.

3. When a map, drawing or chart, etc., was part of the material being photographed the photographer followed a definite method in "sectioning" the material. It is customary to begin photoing at the upper left hand corner of a large sheet and to continue photoing from left to right in equal sections with a small overlap. If necessary, sectioning is continued again — beginning below the first row and continuing on until complete.

4. The majority of users indicate that the textual content is of greatest value, however, a somewhat higher quality reproduction could be made from "photographs" if essential to the understanding of the dissertation. Silver prints of "photographs" may be ordered at additional charge by writing the Order Department, giving the catalog number, title, author and specific pages you wish reproduced.

5. PLEASE NOTE: Some pages may have indistinct print. Filmed as received.

Xerox University Microfilms
300 North Zeeb Road
Ann Arbor, Michigan 48106

THE GENERATION OF OCEAN WAVES BY A TURBULENT WIND

A dissertation submitted to the

Division of Graduate Studies
of the University of Cincinnati

in partial fulfillment of the
requirements for the degree of

DOCTOR OF PHILOSOPHY

in the Department of Physics
of the Graduate School of Arts and Sciences

1973

BY

James H. Stuhmiller

B.S. Massachusetts Institute of Technology, 1965
M.A. Queens' College, 1968

UNIVERSITY OF CINCINNATI

MARCH 28 19 73

I hereby recommend that the thesis prepared under my supervision by JAMES H. STUHMILLER

entitled THE GENERATION OF OCEAN WAVES BY A TURBULENT WIND

be accepted as fulfilling this part of the requirements for the degree of DOCTOR OF PHILOSOPHY

Approved by:

F. Paul Esposito

Louis Witten

M. Gutman

Form 668—Grad. School—1M—8-67

TABLE OF CONTENTS

1 INTRODUCTION

1.1 HISTORICAL INTRODUCTION

One of the issues central to the understanding of the dynamics of the Earth's atmos phere and oceans is the coupling which exists at their interface. The interaction influences both the general circulations of the oceans and the global distribution of climate. However, the most immediate and obvious effect is the generation of surface waves. This phenomena has attracted the interest of workers in fluid mechanics for over a century, but because of the chaotic nature of the sea and the turbulence of the airflow, a theoretical exposition of the process has yet to be discovered.

The attempts to explain wave generation by the winds may be traced to the original papers of Kelvin (1871) and Helmholtz (1868) which treat the instability of a surface across which a tangential discontinuity in velocity exists. For air flowing over water, the interface becomes unstable when the air velocity approaches 660 cm/sec, with the surface forming ripples 1.7 cm in length. It was known, even at that time, that waves can be raised by a

much more gentle wind and that the first waves to appear have considerably longer wavelengths. However, Kinsman (1962) reports that the sea takes on a visually different appearance for wind velocities exceeding 7 m/sec and Wu's (1968) criteria for the separation of airflow from water waves, to be discussed in detail later, also leads to critical airflow velocities near the Kelvin-Helmholtz result. This is just one of the many aspects of the air-sea interaction which is not clearly understood.

Jeffreys (1924,1925) proposed a heuristic model of wind-wave generation, based on the assumed sheltering of the lee side of a growing wave by its own crest. He avoided the problem of the initial instability of the water surface by postulating the existence of already formed waves, considering only how they might continue to grow. The mechanism of energy transfer was an ærodynamic pressure force in phase with the wave slope, caused by flow separation at the wave crest. He chose a form for the pressure force which was proportional to the wave slope, the square of the relative velocity of the wind and wave, and a constant of proportionality, called the "sheltering coeficient". This number was determined by reproducing the known minimum

wind speed. The resulting wavelength and wave speed of the first waves were in reasonable agreement with observation.

It was undertaken by Stanton, et al (1932) to determine this coefficient experimentally. Properties of the airflow over a variety of fixed wavetrain models were measured. The sheltering coefficient, and hence the effect on wave growth, were found to be a hundred times smaller than the value proposed by Jeffreys. Furthermore, Motzfeld (1937), in experiments which determined the detailed flow lines over fixed, wavy models, found that separation did not occur until the air velocity was an order of magnitude greater than the minimum velocity for raising waves. Not only was Jeffreys' theory discredited, but the experiments stood as an indictment of pressure forces, in general, as the agents in wave growth.

The exigencies of beach landings in World War II required that the problem of wave forecasting be solved. So, despite its difficulties, Sverdrup and Munk used Jeffreys' theory in conjunction with a proposed shear force to produce an empirical theory of wave generation and propagation. The results were eventually published as an unclassified

article in 1947. The theory, disussced in detail in Kinsman (1962), was remarkably successful. The reason for this unexpected success is, in part, explained by the present work, wherein the effects of airflow separation are properly taken into account and combined with a mathematical description of turbulent flows.

Following the war, attention turned to the description of the sea surface as a first step in the construction of a more viable theory of generation. The pioneering efforts of Pierson (1952) and Neumann (1952) allowed the mathematics of stochastic processes to be applied to ocean measurements. The result, the Pierson-Neumann theory (1961) extended the Sverdrup-Munk theory to two dimensions, under conditions of gusty, time-varing winds. Eckart (1953) also proposed a theory based in stochastic processes, however, all of these efforts are deeply rooted in empiricism. Ursell (1956), surveying the problem for the G.I. Taylor memorial volume, wrote "Wind blowing over a water surface generates waves in the water by physical processes which cannot be reg arded as known." He emphasized the lack of a deductive theory. The next year two new theories

of generation were published.

Phillips (1957) proposed that a resonance might develop between a surface wave on the water and turbulent pressure fluctuations advected by the mean airflow. The resulting energy transfer is such as to cause the amplitude of the waves to increase as a power of the time. It can be applied to initial wave formation. Phillips estimated the magnitude of the turbulent pressures and applied the result to short-time spectral development. However, as had occured thirty years before, experiment showed the theorist to be overly optimistic. Longuet-Higgins (1962), reporting measurements made in the mid-Atlantic, found the estimated fluctuations too large by a factor of a hundred. Later evidence has also shown that the amplitudes of waves, during their greatest growth, increases exponentially with time. The resonance mechanism does not apply to the growth of already formed waves, but it stands as the only explanation of initial formation, even though it is not quantitatively correct.

Miles' (1957) "inviscid" theory was the first mathematically derivable explanation, involving a minimum of empiricism. It has become the standard against which experiment and other theoretical

work have been compared. The result is based on the fact that laminar, parallel flows, in which the vorticity increases with height, are unstable to small perturbations. The disturbances grow exponentially, with the growth rate being proportional to the curvature of the velocity profile at the point where the air velocity is equal to the phase speed of the wave, the critical level. The result had first been obtained by Tollmein (1929) as an explanation of the transition from laminar to turbulent flow in a boundary layer, and was formalized as part of a general theory of stability by Lin (1955). In Miles' theory, turbulence is taken into account only to the extent that it determines the original velocity profile.

The mathematical foundation of the "inviscid" theory was developed more rigorously in papers by Benjamin (1959), Conte and Miles (1959) and Miles (1959). Benjamin demonstrated the correctness of the boundary conditions assumed and evaluated explicitly the influence of the viscous sublayer, particularly when the critical layer occurs within the sublayer. Conte and Miles made numerical integrations of the Orr-Sommerfeld

equation, the governing equation of motion in the inviscid theory, using a particular, self-consistant velocity profile. They found growth rates three times smaller than estimated in the original paper. Miles then restated the 1957 paper in more elegant mathematics, included the dominant viscous terms in the equations of motion, and obtained the same formal solution as before, with the magnitudes modifies by the results of numerical integration.

In 1962 the limited amount of experimental evidence available seemed to be in agreement with the "inviscid" theory. The results of Stanton, et al (1932) and Motzfeld (1937), which had ruled out pressure mechanisms, could be explained as due to using fixed models which do not allow a critical level to form. Wave growth inferred from spectral data of Sverdrup and Munk (1947) and Longuet-Higgins (1962) supported the theory, at least were not in disagreement. Miles (1960) joined Phillip's resonance theory to his own as an explanation valid at all stages of wave growth. Lighthill (1962), remarking that "...a correctly argued fluid-mechanical theory, a body of comprehensively instrumented and recorded experiments, and a demonstration of the

adequate agreement between the two,...have in large measure been supplied...", offered a physical interpretation of the "inviscid" theory. He argued that at the critical level a closed-streamline pattern forms, moving with the surface wave. This region is called the critical layer. The addition of diffusion to the flow allows the critical layer to transport vertically fluid properties which have gradients in the neighborhood of the critical level. It is the transport of vorticity which leads to the energy transfer predicted in the "inviscid" theory. Although these arguments do not assist in obtaining numerical results, they do expose characteristics of the flow near the critical level and serve as a guide to intuition.

There was, however, a theoretical objection to the "inviscid" theory raised by Stewart (1961). He argued that the energy and momentum transferred to the water, which establishes the initial profile, should to a large extent be due to pressure forces, wave drag, rather than through shear forces as implied in Miles' theory. Stewart advocated that the airflow near the water should be significantly modified by the presence of waves and that this modification invalidates at least the direct

application of the theory. The field measurements of Dobson (1971) confirm Stewart's contention and it is the modified airflow near the water surface which plays an important role in the results derived in this work. In section 2, we obtain analytically many of the features anticipated by Stewart.

In 1966, four experiments were reported, which, for the first time, directly measured wave growth parameters. Shemdin and Hsu (1966) measured the aerodynamic pressure above travelling water waves in the newly-constructed Stanford wind-wave tunnel. The sensor was maintained at a fixed distance above the wave by a mechanical servo-system. The measured pressures were in agreement with those predicted by Miles' theory. Zagustine, et al (1966) measured the growth of waves propagating against a water current, which was such as to make the wave form stationary in the laboratory frame of reference. Their results also supported the theory. However, laboratory measurements of Weigel and Cross (1966) and the ocean measurements of Snyder and Cox (1966) both indicated that the theroy underpredicted the growth rates by as much as a factor of ten. Miles (1967), noting these discrepancies, especially in

the sea measurements, suggested that some scaling effect was at work in the geophysical boundary layer which would increase the predictions by the required amount. This scaling effect could not be justified theoretically, however, and led to other inconsistencies itself (see Davis (1969)). Attempts to include turbulence effects through mixing length theories were made by Miles (1964), Danner (1966) and Long (1970). The former two led to mathematical difficulties which could not be resolved, while the latter was a numerical experiment with many free parameters, chosen to give agreement with a particular experiment. None of these were ever published.

The theory's serious underprediction of the magnitude of the growth rate was confirmed in experiments by Plate, Chang, and Hidy (1969), Kendall (1970), Sutherland (1968), Chang, Plate, and Hidy (1971), Bole and Hsu (1969), and others. The latter investigators repeated the experiments of Shemdin and Hsu (1966), with improved equipment and found that the earlier agreement was unjustified. Finally, very detailed ocean measurements by Dobson (1971) not only showed the underprediction, but clearly indicated that the growth

rate was not a function of the wave age only, as had been predicted. The wave age is the ratio of wave to wind speed. The "inviscid" theory and its simple modifications were finally abandoned, just as the "sheltering" theory of Jeffreys had been abandoned forty years before.

Current research into the generation of ocean waves has centered on obtaining a correct description of the wave-induced turbulence interactions in the air which are neglected in Miles' original theory. Davis (1970) showed that the fluctuating turbulent stresses can play an important role in the energy balance, and that even if the "inviscid" theory were valid, the motions would be dominated by turbulence effects. Some viscoelastic aspects of turbulence have been explored theoretically and experimentally by Hussain and Reynolds (1970) as a method of estimating the influence of wave-like perturbations. Davis (1972,1973) has combined this work and the turbulent boundary layer calculations of Bradshaw, et al (1967) to produce a general model of "turbulence-with-a-memory". He then used this to generate, numerically, flow patterns which might apply to the generation of surface waves. Although indicating that large

growth rates are possible, when compared in detail with the experiments of Kendall and Dobson the results are inconclusive. These and other theories will be discussed in section 4 in relation to the theory developed in this work.

1.2 PLAN OF ATTACK

This work is divided into three major parts. In section 2 the airflow near the water surface is considered. The effects of a distribution of surface waves on the airflow is analysed and formulae are derived in the case of airflow separation. In section 3, we discuss the stability of turbulent flow in the presence of a flexible boundary. It is shown that when gradients in the turbulent stresses exist, energy is transferred from the mean flow to the surface wave causing it to grow. Finally, in section 4, the results of the earlier sections are combined to produce a theory of ocean wave generation. The predictions are found to agree with field measurements within experimental error.

2. THE AIRFLOW OVER WAVES

2.1 GENERAL CONSIDERATIONS

The purpose of this section is to estimate the mean flow quantities in a turbulent boundary layer over water waves. These results, specifically the mean horizontal velocity and the mean turbulent Reynolds stresses, will be combined with the formaulae developed in section 3 to produce expressions for ocean wave growth rates.

A quite adequate estimate of these gradients may be obtained without detailed physical modelling. It is known by direct measurement, that above the waves the mean turbulent Reynolds stresses and the mean horizontal velocity take on nearly constant, non-zero values. At the water surface, because the water has no net horizontal motion and is non-turbulent, both of these quantities must vanish, thus gradients must exist. The region over which the wall strongly influences the airflow is scaled by the average surface roughness, which in this case is the average waveheight. We could infer without further argument, that the required gradients are given approximately by their constant value divided by the average waveheight. It is precisely this

result which will be established.

Another property of the flow, necessary to the evaluation of the formulae of section 3, is the equivalent eddy diffusion coefficient. When a description of turbulence is obtained by averaging moments of the Navier-Stokes equations (the proceedure employed here), each order quantity is expressed in terms of higher order moments. To terminate the process, a closure hypothesis must be invoked. A simple closure, employing the diffusive nature of turbulent flows, allows writing higher moments in terms of gradients of lower ones. For example,

$$\langle u_i u_j u_k \rangle = -\nu_E \frac{\partial}{\partial x_k} \langle u_i u_j \rangle , \qquad (1)$$

where the angular brackets signify the averaging proceedure over which the moments are defined. ν_E is an equivalent eddy viscosity, whose value is to be specified independently. Many theories have been advanced which supply formulae for ν_E, including the mixing length theory of Prandtl, however, here the value can be obtained most readily by considering the connection between the second-order moments, the momentum fluxes, and the first-order moments, the mean velocities. Since the total vertical flux of horizontal momentum may be determined from velocity

profile measurements far above the surface, we may relate this to the gradient in the horizontal velocity. We have

$$\langle u_i u_j \rangle = -\nu_E \frac{\partial}{\partial x_j} \langle u_i \rangle , \qquad (2)$$

which for i=1 and j=2 becomes

$$\tau = \nu_E \frac{dU}{dy} , \qquad (3)$$

where $-\tau$, $\tau > 0$, is the total momentum flux. When U is specified, this becomes a formula for ν_E .

The magnitude of the gradients and the effective viscosity are all that are required to evaluate the general equations of section 3, and thus no further discussion is required to predict ocean wave growth. It is this lack of dependence of the final results on the details of the air-water interaction which insures that the general features of the theory will survive future clarification of the processes of the interface region.

However, there are good reasons for developing a detailed model of the airflow near the water surface at this time. Firstly, many as yet unconnected experimental measurements of the airflow over water

waves, such as separation effects, anomalies in turbulence intensities, and the ratio of wave drag to the total momentum flux, can be brought together in a unified theory. The theory is deductive, which in principle can be used to calculate details of the air-sea interaction. This not only extends the precision of the predictions, but offers secondary tests of the model. As a practical matter, the interconnection of the various aspects of the phenomena reduces the number of parameters necessary to describe the sea and consequently the number which must be measured. Secondly, inherent limitations in the theory obtained may be understood in terms of the detailed processes. The role of wave-driven motions at small wind speeds, the interconnection of growth and wave drag, and the ultimate inapplicability of the theory to low frequency surface waves all fit within the proposed model. Finally, a physical model of the interface region can form a basis from which a study of other processes may begin. For example, over 80% of the energy which drives the Earth's atmosphere is released from latent energy in water vapor. The proper understanding of mass and heat fluxes at the oceans' surface is therefore necessary to the understanding of atmospheric motions.

The present model may play some role in that understanding and may clarify the experimental differences which exist in the present measured values of these quantities.

2.2 AN OVERVIEW OF THE AIR-WAVE INTERACTION

The lower boundary of the atmosphere over the ocean is constantly and randomly heaved by surface waves. The characteristic length scale over which the wave-induced airflow varies is much larger than distances overwhich molecular viscosity is important, thus the flow may be treated as inviscid. To determine the first-order effects of a particular wave component, we need only study those airflow motions which have the same frequency as the wave. This means that a Fourier average must be performed, which, for a stationary and homogeneous statistical spectrum of surface waves, is equivalent to an ensemble average made in the frame of reference in which the waveform of this component is at rest. If it is determined that a pressure in phase with the wave slope exists, the wave will grow and the rate of growth can be calculated. Since we shall only be concerned with the growth of very small waves (waves whose amplitudes are small compared with both the average waveheight of the spectrum and their own wavelength), we shall treat the problem as a perturbation of the mean flow in the absence of the growing wave. It is this mean flow, due to the wind and the large

amplitude waves, which is to be determined.

If the effects of the waves were linear, that is, just the additive resultant of the effects of each frequency component, the ensemble average described above would yield a mean airflow identical to the flow over a smooth wall. However the effects are not linear, for example, wave-breaking and wave-wave interactions are well-documented phenomena. The present model will explore the effects of another non-linear interaction, also directly observed, that of airflow separation from instantaneous wave crests.

When separation occurs (in the airflow around a bluff body in a wind tunnel, say), a wake forms behind the object while the free stream flows around the wake as though it were a solid body. See Figure 1a. The free stream and the wake are joined at a separation streamline, along which the pressure increases rapidly downstream. In the wake, the ambient pressure is low, thus when separation occurs, the drag on the object increases tremendously compared with the non-separated case for the same free stream velocity. The increased force is, of course, the pressure difference between the free stream and the wake. For a single free object, the

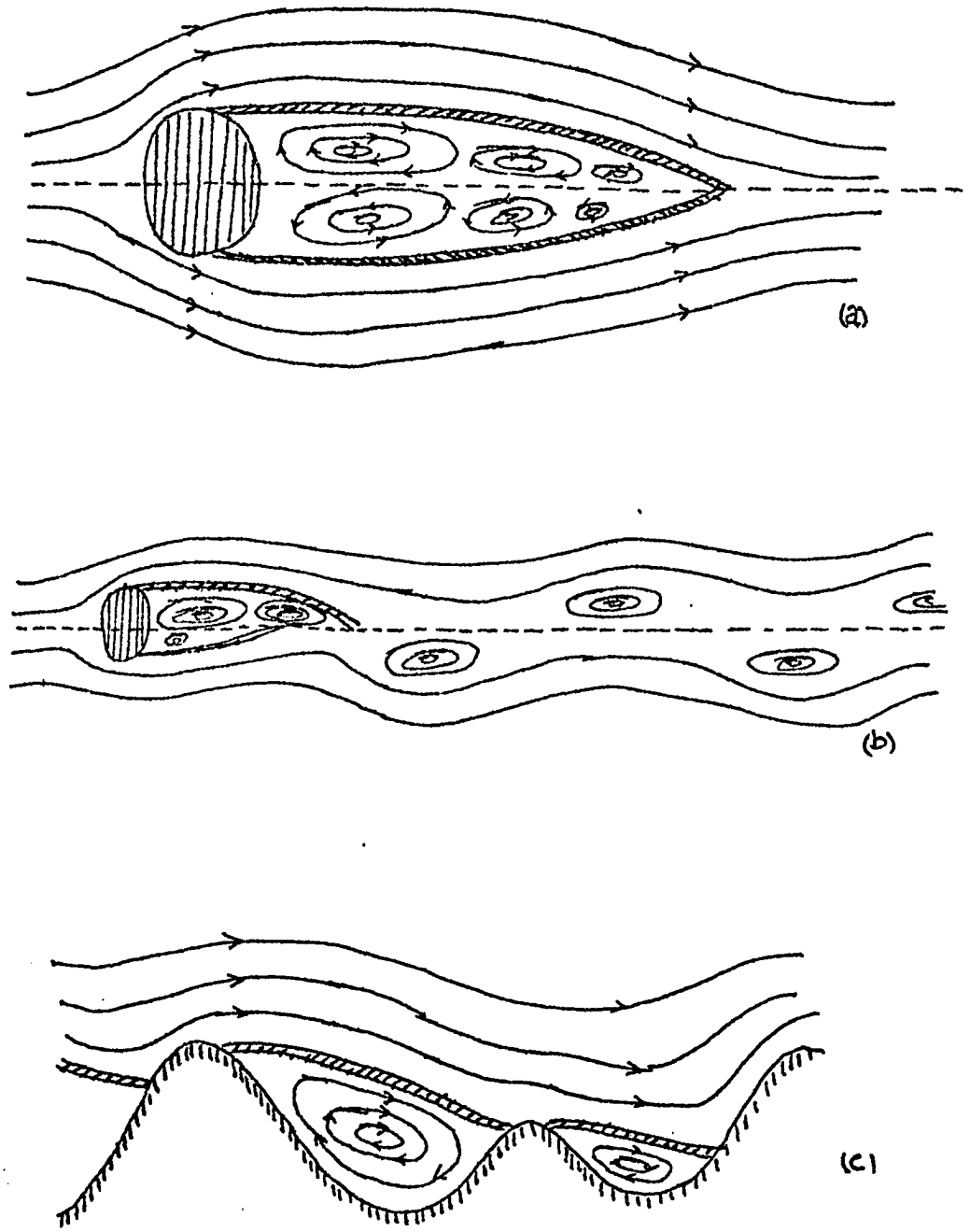

Figure 1. Schematic illustration of flow separation and the formation of a wake. (a) the wake behind a bluff body. (b) wake separation forming a Karman vortex street. (c) reattachment for flow near a wall.

wake becomes unstable and tears itself free of the object, carrying downstream the swirling motion as isolated vorticies. A new wake forms after the detachment and the process continually repeats itself, producing the familiar Karman vortex street. See Figure 1b.

However, for separation from water waves, the close proximity of a wall causes the separation streamline to reattach itself somewhere on the next wave face. See Figure 1c. The free stream, wake, and separation streamline have the same characteristics as for the single free object case. Energy and momentum are lost from the mean free airflow by the formation of the wake, and delivered to the water, as wave momentum and energy, by the pressure difference on the forward and leeward sides. The wake can be torn free in this case, also, by the undulating motion of the surface itself, and, in one theory of wall turbulence, it is the vorticies shed in this process which leads to the observed turbulence of the airflow.

2.3 EXPERIMENTAL SUPPORT FOR SEPARATION

Wu (1970), noting that there was evidence that the drag coefficient over the ocean changed discontinuously at a particular wind velocity, proposed that airflow separation occurred at that speed. He formulated the criterion that "airflow separation occurs from waves having a phase speed less than the shear velocity." Using this criterion he was able to explain Charnock's expression, which relates the shear velocity to the surface roughness, originally proposed on dimensionality arguments. These results were also found to be consistent with the diffusion sublayer thickness as determined by Schooley (1971) from measured evaporation rates over water waves.

Separation will first occur over the slowest moving waves. Because of the opposing effects of surface tension and gravity on the dispersion relation, water waves have a minimum phase speed which occurs for ripples about 2 cm in length. Since these ripples are superimposed on the larger waves of the ocean, which make up the primary contribution to the rms surface displacement, separation will occur at each instantaneous crest

of the surface.

Chang, Plate and Hidy (1971) measured the airflow relative to a particular component of the water wave spectrum generated in a laboratory wind-wave tunnel. They chose to study the dominant wave, that is the largest wave in the spectrum. They determined that separation does occur from the wave crest and Figure 2 , taken from their Figure 6, shows the average streamline pattern relative to the dominant wave. A leeward wake is clearly defined. This firmly established the existence of airflow separation.

Experimental difficulties did not allow determination of the wake flow or even the precise shape of the wake. However, Chang, et al discuss the many similarities of the flow with those measured by Arie and Rouse (1956). of separation in a turbulent boundary layer from a wall projection. Figure 3 , Aire and Rouse's Figure 8, indicattes the wake pattern which developes. One distinctive feature found in both investigations was that the separation streamline was associated with a pronounced maximum in the turbulence intensity. Figure 4a shows the relation between the separation streamline and the $\langle u^2 \rangle$ value at several stations

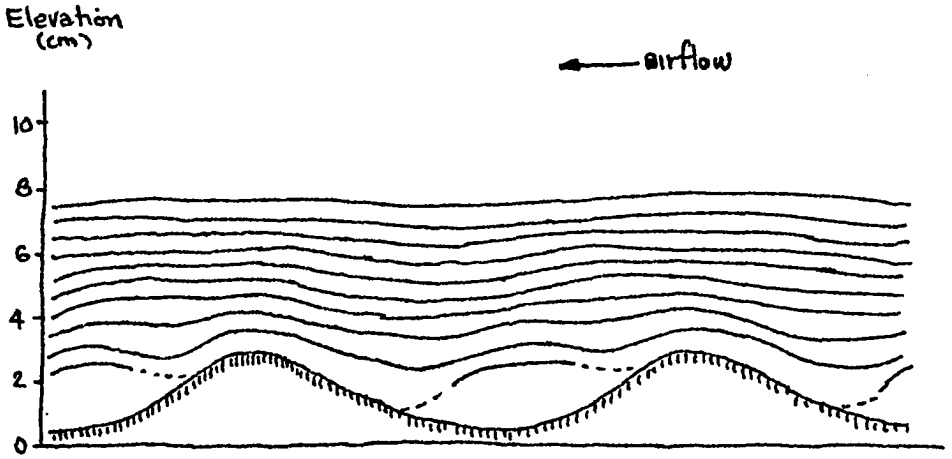

Figure 2. Average streamline pattern of airflow over water waves found by Chang, et al (1971). A leeward wake due to air flow separation is clearly indicated.

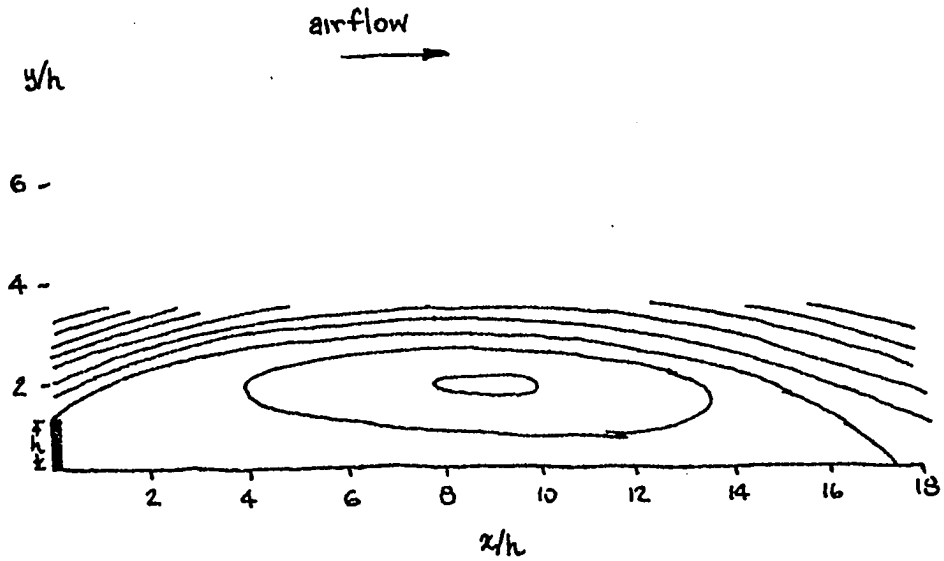

Figure 3. Streamflow pattern in the wake of a wall protrusion which causes airflow separation. From Arie and Rouse (1956).

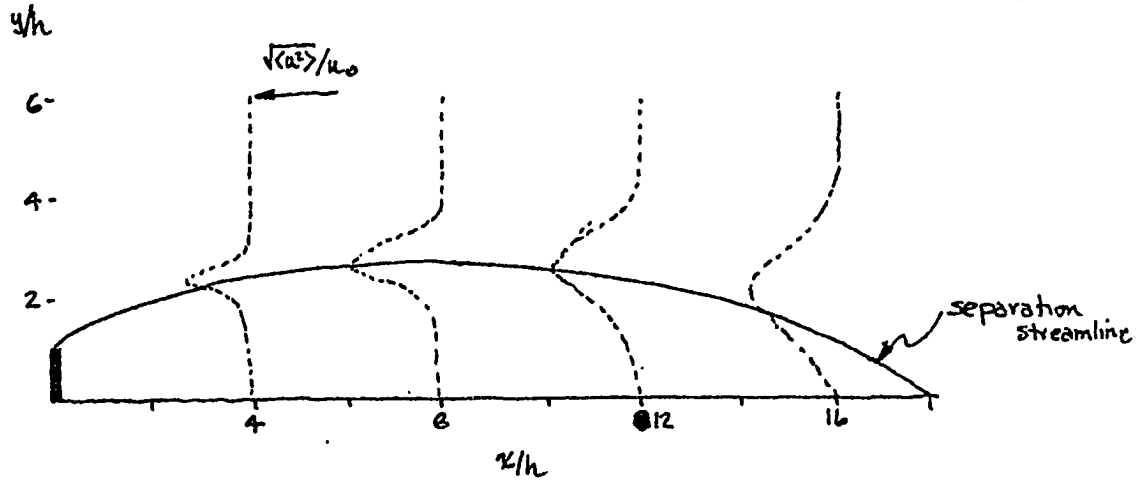

Figure 4a. Measured turbulence intensity downstream of the point of separation caused by a wall protrusion. From Arie and Rouse (1956). The separation streamline corresponds closely to the position of the intensity maxima.

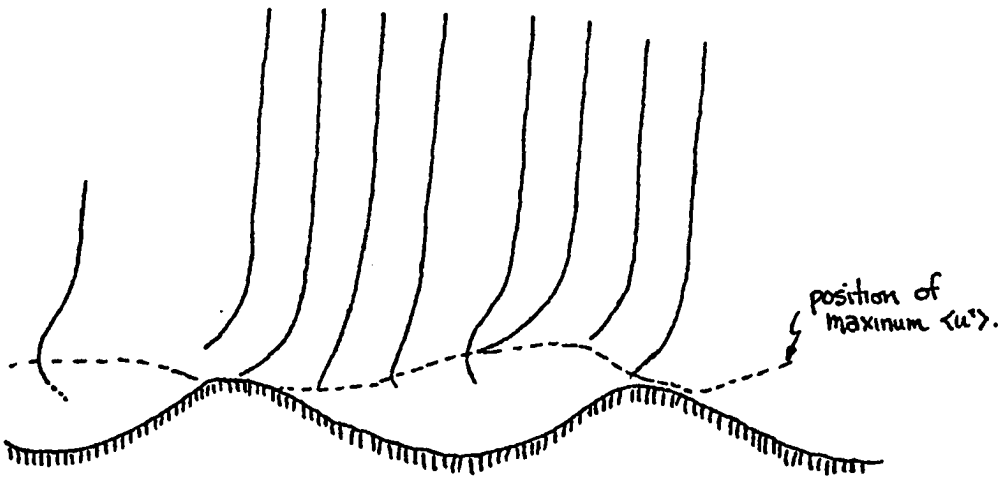

Figure 4b. Measured turbulence intensity above water waves. From Chang, et al (1971). Dotted line indicates the position of the intensity maxima. By analogy with the solid wall case, dotted line also indicates the position of the separation streamline.

along the wall. Based on this measure of the position of the separation streamline, the wake behind the dominant wave is much larger and almost completely fills the region between crests. See Figure 4b .

We have shown that there is direct evidence of airflow separation from the crests of water waves. The nature of the flow is similar to that of separation from fixed protrusions on a wall, which has been well-documented. Depending on the manner in which the separation streamline is inferred, the wake occupies from about half to all of the crest to crest region.

2.4 THE ENSEMBLE AVERAGE NEAR A SURFACE IN RANDOM MOTION

For the description of turbulent flows, it is convenient to define an ensemble average, denoted by $\langle Q \rangle$, which devides each flow quantity into a mean part, denoted by an upper case letter, for which $\langle Q \rangle = Q$, and a fluctuating part, denoted by a lower case letter, for which $\langle q \rangle = 0$. The average is made over an ensemble of all possible flow realizations. We now discuss the nature of the average when flow near a boundary, which itself is in random motion, is considered.

For turbulent flows over fixed boundaries, it is sufficient to average fluid properties at a fixed spatial position and a fixed time over an ensemble of identically prepared flows. If the statistical processes are stationary, as will always be assumed, the average may be taken as a time average. However, two complications arise when a mean flow is defined over water waves, that is, a surface in random motion. Firstly, fixed spatial positions cannot be related to positions above the mean water level, and in fact may not always occur within the same fluid for positions

close to the boundary. The proper generalization is to make measurements at fixed horizontal positions and fixed vertical positions above the instantaneous water surface. This leads to the correctly defined mean coordinates $(x,\bar{y})$. Secondly, the randomness of the airflow, that is, the fluctuations of the airflow parameters from their mean values, reflects two distinct motions: the turbulence of the airflow and the heavings of the water surface. Very near the water, the fluctuations will be due to surface motions, while far above turbulence will dominate. In general, there will be a broad, overlapping region in which the contributions of the two sources will be com-lexly intermixed. However, through an idealization of the effects of separation, we shall be able to distinguish the two effects and perform the necessary averaging in a mathematically simple way.

2.5 EFFECTS OF SEPARATION ON THE MEAN AIRFLOW

Consider the separation from a particular waveform. The free stream is only slightly affected by the geometry of the instantaneous waveform, and then only to the extent that the wave crest determines the height of the separation streamline. Consequently, it is not unreasonable to assume that the flow above the separation streamline (the free flow) has fluctuations which are uncorrelated with the surface waves. Conversely, the wake is geometrically related to the wave, moving with it with an organization which causes the transfer of momentum and energy to the water. This motion is highly correlated with the surface motions. We shall take the separation streamline as dividing the flow into two distinct regions: the free stream flow above the streamline, in which the airflow fluctuations are uncorrelated with repect to the surface, and the wake, between the streamline and the water surface, in which the fluctuations are highly correlated. We then divide all fluid properties into correlated and uncorrelated parts and write

$$q = q_{cor} + q_{unc} \,. \qquad (4)$$

This idealization allows the ensemble average to be formulated simply. Because of the spatial homogeneity of both the turbulence and the surface motions, we may perform the ensemble average by averaging the fluid properties at a fixed time and fixed height above the instantaneous surface over the entire horizontal ensemble.
Thus

$$\langle Q \rangle = \langle Q \rangle_{cor} + \langle Q \rangle_{unc} , \quad (5)$$

where

$$\langle Q \rangle_{unc} = \langle Q \rangle \text{ when } \bar{y} > y_{ss} , \quad (6)$$

and

$$\langle Q \rangle_{cor} = \langle Q \rangle \text{ when } \bar{y} < y_{ss} . \quad (7)$$

We can replace the horizontal average by an average over a "typical waveform" by defining the distribution function $P(\bar{y})$, such that $P(y_{ss})\, dy_{ss}$ is the probability that the separation streamline occurs between y_{ss} and $y_{ss}+dy_{ss}$ above the instantaneous water surface. Since the free stream properties of interest, the

turbulent Reynolds stresses and the horizontal velocity, vary slowly with height, they can be replaced with their constant values $\langle \mathcal{Q} \rangle_0$, and we have simply

$$\langle \mathcal{Q} \rangle_{unc} = \langle \mathcal{Q} \rangle_0 \int_0^{\bar{y}} P(y_{ss})\, dy_{ss}. \qquad (8)$$

We see that the uncorrelated part vanishes at the mean water level as expected. Similarly, the correlated part is given by

$$\langle \mathcal{Q} \rangle_{cor} = \int_{\bar{y}}^{\infty} \langle \mathcal{Q} \rangle\, P(y_{ss})\, dy_{ss}, \qquad (9)$$

where the average may not be taken outside the integral until it is established that it has no dependence on the vertical coordinate. As expected, $\langle \mathcal{Q} \rangle_{cor}$ vanishes far from the surface.

Further simplification is possible by considering the flow quantities individually. Take $\mathcal{Q} = \mathcal{U}$, the horizontal velocity. When there is no wave-driven mean motion, $\langle \mathcal{U} \rangle$ vanishes within the wake and we may write the total mean horizontal velocity as

$$U = \langle \mathcal{U} \rangle = U_0 \int_0^{\bar{y}} P(y_{ss})\, dy_{ss}. \qquad (10)$$

For $\mathcal{Q} = uv$, the shearing Reynolds stress or the vertical flux of horizontal momentum, we have

$$\langle uv \rangle = \langle uv \rangle_0 \int_0^{\bar{y}} P(y_{ss})\,dy_{ss} + \int_{\bar{y}}^{\infty} \langle uv \rangle\, P(y_{ss})\,dy_{ss}. \quad (11)$$

The uncorrelated part may be evaluated from a knowledge of $\langle uv \rangle_0$ and the probability distribution P(y). The correlated part may be written in terms of the uncorrelated part by invoking conservation of momentum. After the average has been performed, the surface waves are no longer part of the flow description, so that the momentum flux must be carried entirely by the mean air motions. Denoting by $-\tau$ the total momentum flux to the water, we have

$$\langle uv \rangle_{cor} + \langle uv \rangle_{unc} = -\tau \quad (12)$$

or

$$\langle uv \rangle_{cor} = -\tau - \langle uv \rangle_0 \int_0^{\bar{y}} P(y_{ss})\,dy_{ss}. \quad (13)$$

We cannot evaluate $\langle uv \rangle_0$ from the present considerations.

For example, it is not correct to set $\bar{y} = \infty$ in the expression for $\langle uv \rangle$ above to obtain the relation

$$\langle uv \rangle(\infty) = \langle uv \rangle_0 \int_0^\infty P(y_{ss}) dy_{ss} , \qquad (14)$$

or

$$\langle uv \rangle_0 = -\tau . \qquad (15)$$

$\langle uv \rangle_{unc}$ is fairly constant over distances of the order of the average wave height, that is, over that region where P(y) is significantly different from zero, so that it may be taken outside the intrgral. However, over large height variations it may vary due to other causes than that of flow separation, the change being such as to bring the value from $\langle uv \rangle_0$ to $-\tau$. Thus $\langle uv \rangle_0$ must be determined in another way. We shall do this by considering the dynamics of the separation forces directly.

Across the separation streamline the horizontal velocity, hence the horizontal momentum, is reduced to zero by the pressure gradients. The momentum lost from the airflow is just equal to the momentum gained by the wave motion, that is, that part of the shear stress due to wave drag, τ_w. We may represent the separation forces by a force/volume, $\mathcal{F}_x$, which acts just at the separation streamline, extracting momentum at the rate of $-\tau_w$. We write

$$\mathcal{F}_x = -\tau_w \delta(\bar{y}-y_{ss}). \qquad (16)$$

If we average over all possible wave forms, we have

$$\langle \mathcal{F}_x \rangle = \int_0^\infty -\tau_w \delta(\bar{y}-\bar{y}_{ss})\, P(y_{ss})\, dy_{ss}, \qquad (17)$$

$$= -\tau_w P(\bar{y}). \qquad (18)$$

This is the apparent mean force seen by the air due to the continual transfer of momentum to the water by the separation pressures. This force can be associated with an average shear stress, $\langle \tau_{xy} \rangle$, hence an average momentum flux, by the relation

$$\langle \mathcal{F}_x \rangle = -\frac{\partial}{\partial y} \langle \tau_{xy} \rangle . \qquad (19)$$

By integration, we find

$$\langle \tau_{xy} \rangle = -\tau + \tau_w \int_0^{\bar{y}} P(y_{ss})\, dy_{ss}, \qquad (20)$$

where we have chosen the constant of integration so that the total momentum flux to the water is just $-\tau$. From this point of view, the correlated air motions

do not appear explicitly. However, it is clear from the conservation of momentum

$$\langle uv \rangle_{unc} + \langle \tau_{xy} \rangle = -\tau, \tag{21}$$

that

$$\langle \tau_{xy} \rangle = \langle uv \rangle_{cor}, \tag{22}$$

$$\langle uv \rangle_o = -\tau_w. \tag{23}$$

The explicit form of the turbulent shear stress is then

$$\langle uv \rangle_{unc} = -\tau_w \int_o^{\bar{y}} P(y_{ss})\, dy_{ss}. \tag{24}$$

2.6 EXPLICIT SEPARATION PROBABILITY DISTRIBUTION

The probability distribution P(y) cannot be determined for an arbitrary wave distribution solely from the rms surface displacement, nor can it be found without knowing the details of the separation geometry. However, the following idealization is expected to contain many of the statistical features of the actual sea surface. Let the surface displacement be represented by a single-frequency wave of amplitude $\sqrt{2}\sigma$, where σ is the rms surface displacement. The separation streamline is then taken as a straight line joining the upwind crest and (a) the next crest, (b) the midpoint above the mean water level, or (c) the mean water level. Figure 5 illustrates the envisiaged situations. We expect case (a) to be approached at high wind speeds. The proability distribution may be readily calculated for each of these cases.

Consider case (a). Here, P(y) may be obtained by analytical techniques. By its definition, $\int_0^{\bar{y}} P(y)dy$ is the probability that the separation streamline occurs closer to the instantaneous surface than $\bar{y}$. From Figure 6a we can see that this probability is just $\Delta x/(\pi/2)$, where Δx is the

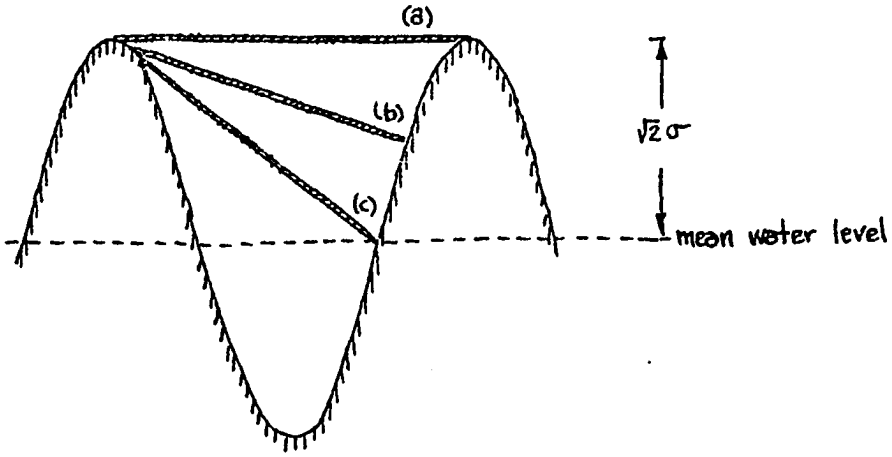

Figure 5. An idealization of the statistical properties of the ocean surface and the geometry of the separation streamline. The surface is represented by a single frequency sinusodial wave whose amplitude is equal to the average wave amplitude, $\sqrt{2}\,\sigma$. Straightlines (a), (b), and (c) represent three possible separation streamline configuarations. Case (a) is expected to be approached at large wind velocities or in the limit of closely packed wave crests.

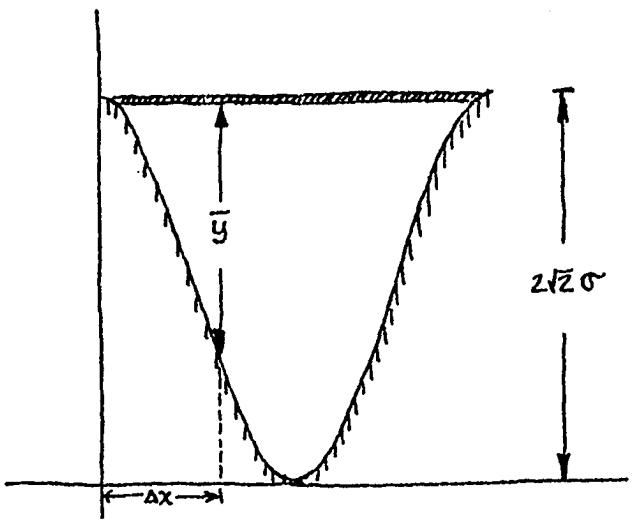

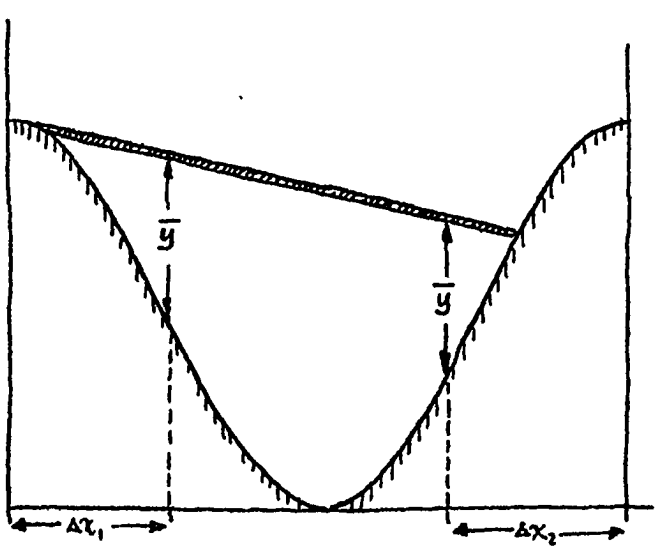

Figure 6. Geometry for calculating $\int_0^{\bar{y}} P(y_{ss})dy_{ss}$.

horizontal distance, measured from the wave crest, at which the waveform and the separation streamline are separated by $\bar{y}$. In general,

$$y_{ss} = \sqrt{2}\,\sigma - \sqrt{2}\,\sigma \cos\chi, \qquad (25)$$

gives the distance between the two lines. Using the multiple angle formula, we find

$$y_{ss} = 2\sqrt{2}\,\sigma \sin^2(\chi/2), \qquad (26)$$

so that

$$\Delta\chi = \sin^{-1}\left(\bar{y}/2\sqrt{2}\sigma\right)^{1/2}, \qquad (27)$$

and

$$\int_0^{\bar{y}} P(y)\,dy = \frac{2}{\pi}\sin^{-1}\left(\bar{y}/2\sqrt{2}\sigma\right)^{1/2}. \qquad (28)$$

We may now evaluate $\langle a\rangle_{und}/a_0$ for case (a). The result is plotted as curve (a) in Figure 7. Cases (b) and (c) are found in the same way: by determining the fraction of the horizontal axis over which $y_{ss} < \bar{y}$. However, the algebraic forms cannot be inverted in these cases to give Δx in terms of $\bar{y}$.

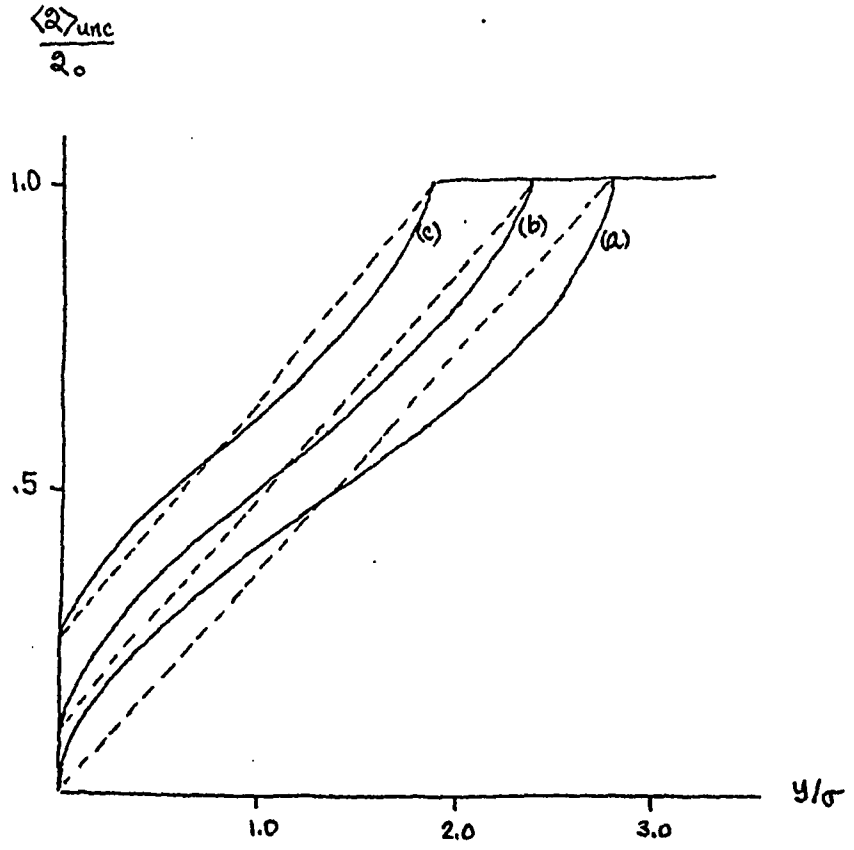

Figure 7. The variation of the uncorrelated mean flow properties with height, calculated from the three separation geometries shown in Figure 6. The dashed curves are straight line approximations. The linear approximations each have the slope $(2\sqrt{2}\sigma)^{-1}$.

Instead, the relation between the two must be determined graphically. Referring to Figure 5b we have

$$\int_0^{\bar{y}} P(y)\,dy = \frac{\Delta\chi_1 + \Delta\chi_2}{\pi} . \qquad (29)$$

The solutions found by these graphical methods are plotted as curves (b) and (c) in Figure 6.

The three cases are closely fit by straight lines, shown as dotted in Figure 7. The lines have slopes which are indistinguishable from one another and lead to gradients in $\langle Q \rangle_{unc}$ equal to the freestream value divided by the average wave height, $2\sqrt{2}\,\sigma$. Thus, our original estimates of the magnitude of the gradients are confirmed. In the formulae to be developed for ocean wave growth, only the magnitude of the gradients appear, so that the exact streamline form does not affect the results. When the separation streamline connects the wave crests, as might occur for high wind speeds or over closely packed wave crests, the thickness of the linear region approaches the average waveheight. We now demonstrate that there is indirect experimental support for this result.

2.7 EXPERIMENTAL CONFIRMATION OF MEAN AIRFLOW DUE TO SEPARATION EFFECTS

The existence of airflow separation from the wavecrest is an experimentally verified result and has been discussed in detail in section 2.3. In this subsection, we wish to discuss evidence that the effects of the separation lead to modifications of the mean flow predicted by the specific model of the last section. Another test, of course, is the comparison of the predicted ocean wave growth discussed in section 4.

Due to experimental difficulties, no measurements within the separated region over water waves have been made. However, near a smooth wall, the mean velocity and the mean turbulent stresses vary linearly with height and the turbulent intensity shows a pronounced maximum at the edge of the linear region (c.f. Figure 8). This is exactly the variation with height predicted for flow over water waves. We shall use this similarity to infer the thickness of the linear region. The flows in the two linear regions can be made identical by scaling the vertical distances by the characteristic lengths associated with the nature of the wall: for a

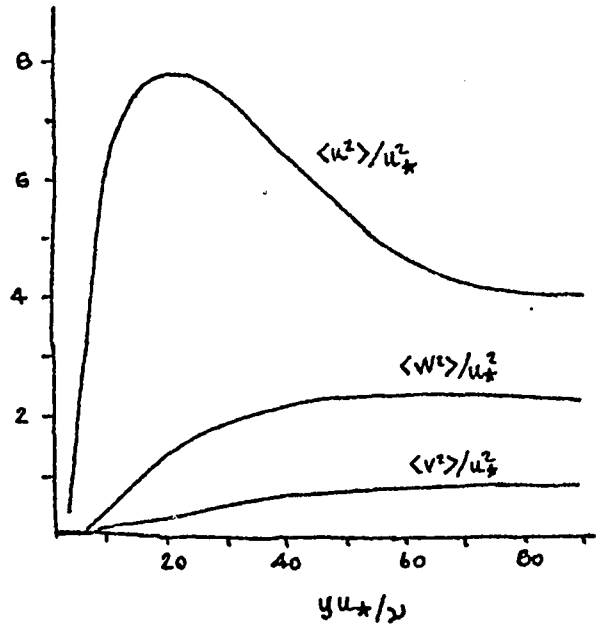

Figure 8. Turbulent Reynolds stresses near a smooth, solid wall as measured by Schubauer (1954). Illustrated is a region next to the wall (y=0) over which the stresses vary linearly with y. The turbulence intensity $\langle u^2 \rangle$ shows a pronounced maxima at the edge of the linear region.

smooth wall, this length is proportional to the kinematic viscosity divided by the shear velocity; for water, it is proportional to the rms surface displacement. The flows external to the linear region are not influenced by the wall mechanism and are scaled only by the geometry determining the boundary layer thickness, δ . If the average waveheight does represent the thickness of the linear region, then we would expect the flow parameters to coincide not only within the linear region, but external to it, when vertical distances are measured away from the edge of the linear region and scaled by δ . The circles in Figure 9 indicate the measured values of the turbulent stress $\langle u^2 \rangle$ found by Plate, Chang, and Hidy (1969) over water waves at high air velocities. The vertical distances have been measured away from the average waveheight $\approx$ .85 cm. The solid lines in Figure 9 are the turbulent stresses measured by Klebanoff (1954) over a smooth wall. The agreement is seen to be quite close. These two sets of data have not been reconcilable until now, because the large thickness of the linear region over water waves was not realized.

Another indirect confirmation comes from

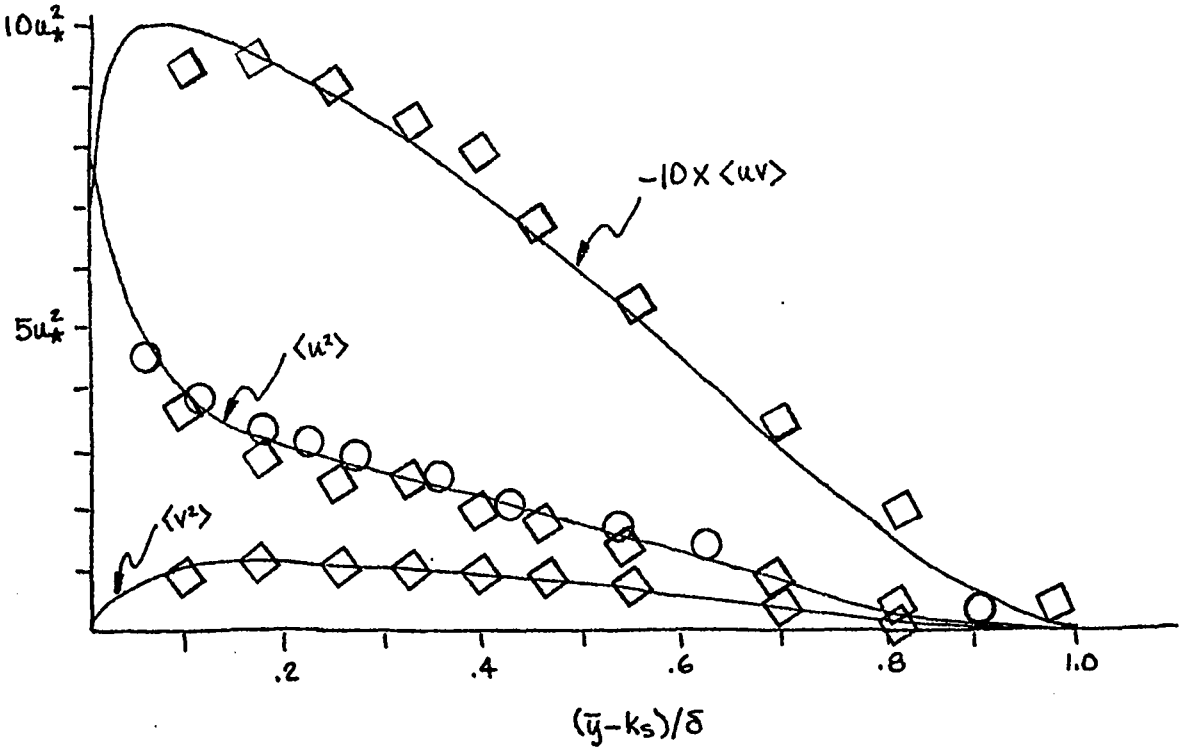

Figure 9. Comparison of the turbulent Reynolds stresses in the airflow over smooth walls (the solid lines) as measured by Klebanoff (1954), over rough walls (◇) as measured by Corrisin and Kistler (1954), and over water waves (O) as measured by Plate, Chang, and Hidy (1969). The coincidence of the data when the vertical distance is measured away from the average surface roughness supports the contention that the thickness of the wall region over water waves is given by the average waveheight.

comparison of the mean velocities exterior to the linear region. Above a smooth wall, a rough wall, or water waves, the mean velocity varies logarithmically with height. Historically, a distance k_s has been defined such that the velocity in this region may be written

$$U = 2.5\, u_* \ln(\bar{y}/k_s) + 8.5\, u_* . \qquad (30)$$

In very extensive measurements of turbulent flows over roughened walls, Nikaruse, reported in Schlichting (1961), found that for very rough walls the velocity profiles took on the above form when k_s was the average surface roughness. Thus k_s is a measure of the extent of the influence of the wall mechanism. This is verified directly in the flow over smooth walls, where the k_s value determined from the velocity profile corresponds to the thickness of the linear region as determined by direct turbulent stress measurements. Extending the analogy, we might expect k_s, determined from the velocity profile above the waves, to indicate the thickness of the linear region over water waves, too. Wu (1968) has made detailed measurements of the air velocity profiles over water waves in the

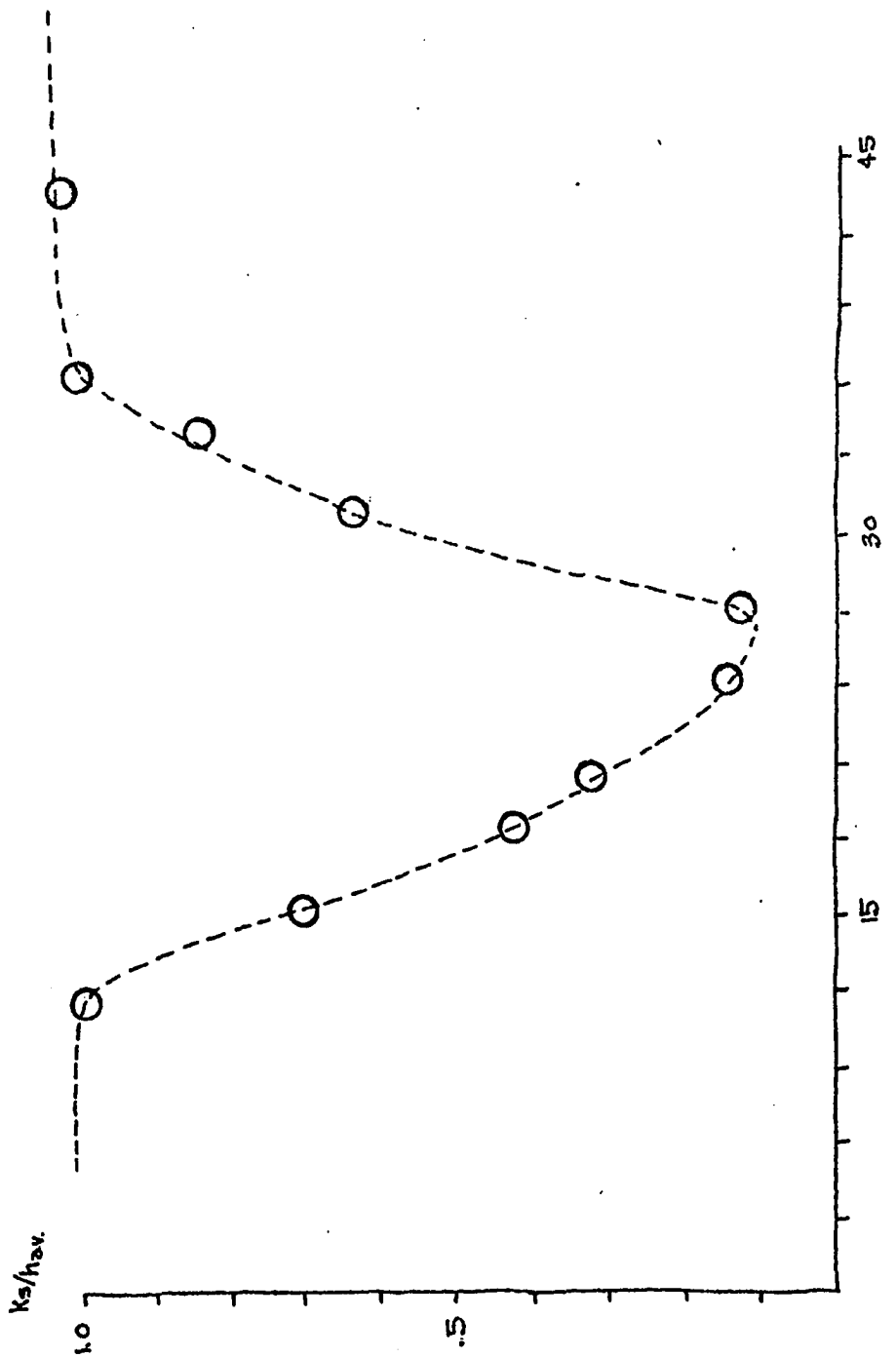

Figure 10.

laboratory and thesimultaneous measurements of their average height. His results are shown in Figure 10. At high wind speeds, k_s is given by the average waveheight as was expected. This relation also holds at low wind speeds, where the wave crests are more closely packed due to the dominance of capillary waves. It is not known whether the deviation from k_s being the average waveheight at middle wind speeds is a real phenomena or a peculiarity of the laboratory situation.

In the absence of direct measurement, comparison with smooth wall measurements indicates the existence of a linear region over water waves whose thickness is given by the average waveheigth. This relation surely holds at high air velocities and may hold under all conditions that large waves exist.

2.8 TRANSPORT PROCESSES IN TURBULENT FLOWS

Whenever averages are employed to produce a mean flow, the random fluctuating motions are necessarily supressed. But, just as in the kinetic theory of fluids, these motions make the mean flow appear diffusive in nature, by causing mixing of properties in adjacent fluid elements. In this section, we shall discuss the analogy between transport by turbulent motions and transport by molecular motions. This is the simplest way in which the gross properties of turbulence can be understood, but it by no means is the only, nor completely correct. A more extensive discussion of this material may be found in chapter 5 of Hinze (1959).

Consider the transport of a fluid property, such as energy or momentum in a turbulent flow of an incompressible fluid. If the quantity considered is not a scalar, we imagine that we are considering a single component. The conservation of the quantity $\mathcal{Q}$ in the motion is given by

$$\frac{\partial}{\partial t}\mathcal{Q} + u_i \frac{\partial}{\partial x_i}\mathcal{Q} = \frac{\partial}{\partial x_i}\left(\kappa_{\mathcal{Q}} \frac{\partial}{\partial x_i}\mathcal{Q}\right) + \mathcal{F}_{\mathcal{Q}}, \qquad (31)$$

where κ_Q is the molecular transport coefficient of $\mathcal{Q}$ and $\mathcal{F}_Q$ represents any sources. If we assume that κ_Q is constant and if we put

$$\mathcal{Q} = Q + q \quad , \quad \mathcal{U}_i = U_i + u_i \, , \tag{32}$$

then we obtain, after the averaging proceedure,

$$\frac{\partial}{\partial t} Q + U_i \frac{\partial}{\partial x_i} Q = \frac{\partial}{\partial x_i} \left(\kappa_Q \frac{\partial}{\partial x_i} Q - \langle u_i q \rangle \right) + F_Q \tag{33}$$

The average $\langle u_i q \rangle$ enters the conservation equation for the mean value of the quantity in exactly the same way as the molecular diffusion. By analogy, we can write

$$- \langle u_i q \rangle = \nu_Q \frac{\partial}{\partial x_i} Q \, , \tag{34}$$

where ν_Q is the turbulence-transport coefficient. This quantity is also called the eddy diffusion coefficient, because the fluctuations can be associated with "lumps" of swirling motion or eddies. The minus sign in this relation not only proceeds by analogy, but also by the stability requirement that irregularities (gradients in fluid properties) tend to be decreased by random motion.

We may derive explicitly the governing equations when $\mathfrak{a}$ is the velocity or momentum of the flow by averaging the equations of motion or the equations of motion multiplied by the velocity. This will be done in section 3. The transport expressions associated with these quantities are

$$-\langle u_i u_j \rangle = \nu_{v_j} \frac{\partial v_j}{\partial x_i} , \qquad (35)$$

and

$$-\langle u_i u_j u_k \rangle = \nu_{v_j v_k} \frac{\partial}{\partial x_i} \langle u_j u_k \rangle . \qquad (36)$$

The maximum utility of this approach (or the minimal external theory which must be added) is achieved if ν_{v_j} and $\nu_{v_j v_k}$ are the same. We first consider this question for molecular transport.

The assumption that molecules behave like rigid spheres leads to the same quantitative results for the various transport coefficients: viscosity, conductivity, diffusion, etc. But corrections are necessary to take into account the elasticity of the spheres, repellent forces, persistency of velocities after collision, and so on, effects which are different in the cases of mass,

momentum, and energy, and the coefficients become unequal. Thus the equality of the coefficients depends on the extent to which the underlying structure is understood.

In Prandtl's momentum-transport theory and Taylor's vorticity-transport theory, ν_{v_j} and $\nu_{v_j v_k}$ are equal (for plane flow). Experiment shows that the result holds only in fully turbulent regions, and then only approximately. This is analogous to the Prandtl number (kinematic viscosity/ thermal conductivity) being also near 1 for gasses.

In the regions of interest for the oceanographic problem, the airflow remains fully turbulent so that

$$\nu_{v_j} = \nu_{v_j v_k} = \nu_\epsilon \,, \qquad (37)$$

is to a large extent justified. Moreover, our immediate goal is to understand the <u>influence</u> of turbulence on wave-induced motions, so that a simple description in terms of the diffusive nature of turbulence is in keeping with the spirit of the investigation. Further refinements must first be justified by the soundness of more basic assumptions.

2.9 EFFECTS OF A SMALL BOUNDARY PERTURBATION

We now consider the effect of a small perturbation of the water surface on the mean flow just obtained. The mathematical consequences will be developed in detail in section 3. Here, we will establish that it is the uncorrelated parts only which are aff ected by the perturbation.

To determine the effect of a small wave, we must view the instantaneous flow. Figure 11 shows a large amplitude waveform on which a small sinusodial wave has been added. As we have already argued, the separation streamline and the free flow above are not affected by the details of the waveform, and thus are not changed by the waviness added to the already irregular waveform. However, the instantaneous surface now varies with the wave so that

$$\bar{y}_{new} = \bar{y}_{old} + a \cos kx . \qquad (38)$$

Thus if a particular streamline was parallel to the mean water surface ($\bar{y}$=0) before the perturbation was applied, it will afterward vary sinusodially in its distance from the mean surface. This is simply

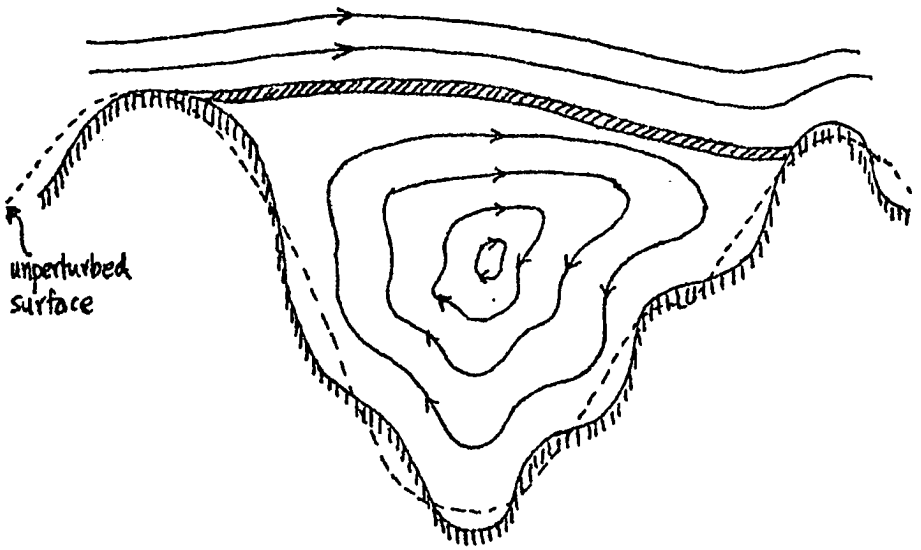

Figure 11. Illustration of the effects of a small disturbance to the instantaneous water surface on the air flow. In accordance with the idealization of section 2.4, that the free stream is influenced primarily by the separation streamline and not the detailed instantaneous surface, the free flow is unchanged by the small disturbance. The wake, on the other hand, conforms to the new surface, again following the ideas of section 2.4 that the wake is completely correlated with the water surface. When the ensemble average is performed, only the free stream, uncorrelated parts of the mean flow will be altered by the small wave.

the statement that the free flow, that is the uncorrelated parts of the flow, see the boundary perturbed from $\bar{y}=0$ to $\bar{y}=a\cos(kx)$. (Remember that the perturbation is stationary in this frame of reference).

The wake flow, on the other hand, must instantaneously match the surface, as shown in Figure Thus there is no effect on the correlated parts after averaging, since both the modified wake flow and the modified vertical distance vary together. One would also be led to this conclusion by considering the apparent stress instead of the correlated motions. This stress depends on the wave drag, the momentum flux to the large waves and on the statistical properties of the large wave spectrum. To the extent that these are unchanged by a small wave, the apparent stress is unchanged.

The effect on the averaged flow of a small perturbation to the boundary is to cause the average boundary seen by the uncorrelated parts to be modified while leaving the correlated parts unchanged.

2.10 SUMMARY

In this section we have considered the mean airflow over water waves. From general arguments, we expect there to exist an inviscid region of influence of the waves of thickness equal to the average waveheight across which the free stream values of the mean horizontal velocity and mean turbulent Reynolds stresses decrease to zero.

We then developed a detailed model of the airflow, taking into account the effects of separation at the instantaneous wave crests. Experimental evidence for separation was reviewed and it was shown that the wake occupies a large fraction of the region between crests. The average over ensembles was discussed in the case when both the air and the water surface were in randon motion. Using the idealization that the separation streamline divides the flow into regions in which the fluctuations are correlated and uncorrelated with the water surface, formule for the mean flow properties were deduced. A simple model of the statistical nature of the ocean surface, a constant amplitude sinusodial wave, was then used to obtain explicit forms for the mean horizontal velocity and the mean Reynolds stresses. Each quantity was found to increase linearly with

height. It was shown that there was indirect support experimentally for this result. Finally, the effects of a small perturbation on this averaged flow was discussed and it was determined that after averaging, only those parts uncorrelated with the surface would be effected by the disturbance.

3 THE STABILITY OF TURBULENT FLOWS NEAR A WALL

3.1 INTRODUCTION

In this section we consider the stability of turbulent flows to perturbations caused by small, travelling waves on the boundaries. We shall have in mind the eventual application to geophysical problems of ocean wave generation, but the results obtained here are quite general and independent of the considerations of the previous section.

Our goal is to determine the interaction of wave-induced motions, caused by the perturbation to the boundary, and turbulence. The approach taken here is to consider both as perturbations, described by ordering parameters ϵ_w and ϵ_T. The fluid properties are expanded in powers of these paramenters. The $O(\epsilon_w \epsilon_T)$ flow represents the interaction to lowest order, and, it will be shown, leads to an instability of the mean motion in which momentum and energy are continually transferred to the surface wave.

The mathematical description is made completely in terms of mean flow quantities by making ensemble averages of the equations of motion. Closure is

achieved by relating third-order velocity correlations to derivatives of the second order correlations, through the description of eddy diffusion along gradients. The flow is assumed to be fully turbulent throughout the region of interest, so that molecular viscosity may be neglected. It is further assumed that the flow is incompressible and two-dimensional.

The critical level, the height at which the mean flow velocity is equal to the phase speed of the disturbance, plays two important roles in the theory. Firstly, it is shown that it is only the value of the fluid properties at the critical level which are involoved in the energy transfer to the wave. Thus, in the limit of the linear theory, one need only concentrate on the description of the flow near this height. Secondly, the wave-induced flow in the neighborhood of the critical level causes a closed-streamline pattern to develop, the critical layer. The diffusivity of the turbulent flow allows the critical layer to transport fluid properties which have gradients in the vicinity of the critical level. This transport, specifically of the turbulent Reynolds stresses, cuases pressures, which transfer energy

and momentum to the wave.

3.2 WAVE RESPONSE TO AN APPLIED PRESSURE DISTRIBUTION

Since we anticipate that the mechanism of instability will be via pressure forces, we establish the connection between the growth rate of a small wave and an applied pressure distribution.

Let the water, or in general the heavier fluid, occupy the half space $y < 0$. The water may be considered as irrotational and incompressible so that the velocity may be derived from a potential function

$$u_i = \frac{\partial}{\partial x_i}\Phi, \tag{39}$$

where ϕ satisfies

$$\nabla^2\Phi = 0. \tag{40}$$

Further, we assume that the growing waves may be decomposed into Fourier components, the equation for the surface of a given frequency component being given by the real part of the equation

$$y = a e^{ik(x-ct)}, \qquad (41)$$

where a is the wave amplitude, k is the wavenumber, and c is the wave speed, in general complex. The boundary condition on the vertical velocity at the surface is then

$$v_s = -ikac\, e^{ik(x-ct)}. \qquad (42)$$

The solution of Laplace's equation, bounded as $y \to -\infty$, and satisfying the boundary condition (42) is, to first order in (ka),

$$\phi = -iac\, e^{ky}\, e^{ik(x-ct)}. \qquad (43)$$

From the velocity potential we may calculate the pressure, p, by

$$-\frac{p}{\rho_w} = \frac{\partial \phi}{\partial t} + gy + \tfrac{1}{2}|\nabla\phi|^2, \qquad (44)$$

where ρ_w is the density of water and g is the acceleration due to gravity. Using the solution (3) and neglecting quantities of order $(ka)^2$, we find that (4) evaluated on the surface yields

$$\frac{P_s}{\rho_w} = (kac^2 - ga)\, e^{ik(x-ct)}, \qquad (45)$$

where P_s is the pressure on the surface due to the airflow, since in the absence of surface tention and viscosity, the pressure is continuous across the boundary. We write P_s is the form

$$P_s = \rho_a c_R^2 (ka)(\alpha + i\beta)\, e^{ik(x-ct)}, \qquad (46)$$

where α and β are the dimensionless values of the pressure at the surface in phase with the surface displacement and slope, respectively.

Dividing this expression by ρ_w, equating the two forms of P_s/ρ_w, and cancelling the common exponential factors, we obtain

$$kac^2 - ga = \left(\frac{\rho_a}{\rho_w}\right) c_R^2 (ka)(\alpha + i\beta). \qquad (47)$$

Writing

$$c = c_R + i\, c_I, \qquad (48)$$

we have, on expansion,

$$c_R^2 + 2i\, c_R c_I - c_I^2 - g/k = \frac{\rho_a}{\rho_w} c_R^2 (\alpha + i\beta). \qquad (49)$$

Equating the real and imaginary parts of this expression, we find

$$c_R^2 - c_I^2 - g/k = \left(\frac{\rho_a}{\rho_w}\right) c_R^2 \alpha, \qquad (50)$$

$$2c_R c_I = \left(\frac{\rho_a}{\rho_w}\right) c_R^2 \beta, \qquad (51)$$

from which

$$c_I = \left(\frac{\rho_a}{\rho_w}\right) \tfrac{1}{2} \beta c_R. \qquad (52)$$

Since $s = (\rho_a / \rho_w)$ is very small, c_I is very small. Thus, to lowest order in s, the first expression becomes

$$c_R = (g/k)^{1/2}, \qquad (53)$$

and then

$$c_I = \tfrac{1}{2} s \beta (g/k)^{1/2}. \qquad (54)$$

The fractional change in the energy of the wave, per radian of its periodic motion is given by

$$\zeta = 2c_I / c_R, \qquad (55)$$

which upon using the explicit forms for the velocities becomes, simply,

$$\tau = \beta s , \qquad (56)$$

where $\underline{c}$ is now and hereafter taken to be the real part of the wave speed. The problem of wave growth rate is then reduced to determining the aerodynamic pressure in phase with the wave slope.

3.3 A DESCRIPTION OF TURBULENCE AS A PERTURBATION

Previous work has revealed the effects of a surface wave on a sheared airflow. The shearing need not be considered as due to turbulence, since for an inviscid fluid, any parallel flow satisfies the equations of motion. We shall consider that turbulence acts as a perturbation which modifies the wave-induced flow and calculate the lowest order correction which results. Let $\epsilon_w = ka$ be a measure of the perturbation caused by the wave and let ϵ_T be a (formal) ordering parameter indicating the magnitude and influence of the turbulence. We shall expand all mean flow quantities in powers of these parameters. O(1) quantities are those which exist in the absence of the wave and turbulence: the original velocity profile. $O(\epsilon_T)$ quantities are those turbulence quantities which exist in the absence of the wave: the original turbulent Reynolds stresses, both correlated and uncorrelated. $O(\epsilon_w)$ quantities are those perturbations caused by the wave alone: we shall sœ that these are associated with the flows of the "inviscid" theory. $O(\epsilon_w \epsilon_T)$ quantities are those perturbations due

to the interaction of the turbulence and the wave, and are precisely the effects neglected in the "inviscid" theory. We shall not consider any higher order perturbations.

This approach to turbulent interactions is unique to this theory. It is normally assumed that the influence of turbulence dominates the flow processes, rather than acting as a perturbation as in this approach. This is necessary to be able to derive from a specific model of turbulence the connection between the original mean velocity and mean turbulent stresses. When the flow is perturbed all aspects of the turbulence and its influence must be considered, resulting in a set of equations which requires many closure hypotheses to be determinant, and even then can only be solved numerically. Here, the original flow, both velocity and stresses are assumed given and the single property of turbulence, that of diffusion, is isolated by the perturbation technique for study. As opposed to other theories incorporating turbulence, we obtain here analytical, closed-form results, in which all parameter dependence is explicit. Also, since only one closure hypothesis is required, there are no free parameters which must be supplied from outside the theory.

3.4 EQUATIONS OF MOTION FOR TURBULENT FLOW

The equations of motion for an inviscid, constant density fluid may be written

$$\frac{\partial}{\partial t} u_i + \frac{\partial}{\partial x_j}\left[u_i u_j + \frac{1}{\rho_a} P \delta_{ij} \right] = 0. \qquad (57)$$

The ensemble average of this equation is

$$\frac{\partial}{\partial t} U_i + \frac{\partial}{\partial x_j}\left[U_i U_j + \langle u_i u_j \rangle_{uncor} + \langle u_i u_j \rangle_{cor} + \frac{1}{\rho_a} P \delta_{ij} \right] = 0, \qquad (58)$$

where we have written the turbulent stresses due to the correlated and uncorrelated motions separately. We note that the correlated stress may be replaced in terms of the apparent stress due to the transfer of momentum to the water.

The continuity equation for an incompressible fluid is

$$\frac{\partial}{\partial x_j} u_j = 0. \qquad (59)$$

Linearity of this equation guarantees that the mean and fluctuating velocities of all orders will be divergence-free. We may then derive the mean velocity from a streamfunction ψ, such that

$$U = \frac{\partial \psi}{\partial y} \quad , \quad V = -\frac{\partial \psi}{\partial x} \, . \tag{60}$$

In addition, the perturbations to be considered are linear in ϵ_w, so that there will be no wave-wave interactions. Therefore, we may consider only those perturbations with the same frequency as the surface wave, separating the coordinate dependence of each flow quantity. The perturbation expansions are then written

$$\psi = \int^y U(\xi)\, d\xi + \epsilon_w \phi^{(1)}(y)\, e^{ik(x-ct)} + \epsilon_w \epsilon_T \phi^{(2)}(y)\, e^{ik(x-ct)} + \cdots \, ,$$

$$\frac{1}{\rho_a} P = \epsilon_w \pi^{(1)}(y)\, e^{ik(x-ct)} + \epsilon_w \epsilon_T \pi^{(2)}(y)\, e^{ik(x-ct)} + \cdots \, ,$$

$$\langle u_i u_j \rangle_{unc} = \epsilon_T \langle u_i u_j \rangle^{(0)}(y) + \epsilon_w \epsilon_T \langle u_i u_j \rangle^{(1)}(y)\, e^{ik(x-ct)} + \cdots \, , \tag{61}$$

where we have made use of the parallel nature of the original flow. Since the correlated quantities are not changed by a slowly growing wave, they have no perturbation terms and the adjective "uncorrelated" need not be retained.

The perturbations must make the wavy surface

a streamline. Since this condition must be met even in the absence of turbulence, we require the $\epsilon_w, \epsilon_w^2, \epsilon_w^3, \ldots$ perturbations to satisfy the corresponding order boundary conditions, while all other perturbations vanish on the surface. From (42) we obtain

$$\phi_s^{(1)} = c/k \quad , \quad \phi_s^{(2)} = 0 \quad , \qquad (62)$$

where the subscript $\underline{s}$ indicates that the quantity is to be evaluated on a suface just outside the viscous subleayer.

Since the water is assumed non-turbulent, all perturbations to the Reynolds stresses must vanish on the surface.

3.5 RELATION BETWEEN THE SURFACE PRESSURE AND PERTURBATIONS AT THE CRITICAL LAYER

In this section we shall establish that the only part of the flow important to the surface pressure in phase with the slope, hence the energy transfer to the surface wave, is that in the neighborhood of the critical level. It is shown that Miles' "inviscid" theory is a special case of this result.

Substituting (61) into (58) we find that the $O(\epsilon_w)$ equations are

$$(U-c)\dot{\phi}^{(1)} - \dot{U}\phi^{(1)} + \pi^{(1)} = 0 , \qquad (63)$$

$$k^2(U-c)\phi^{(1)} + \dot{\pi}^{(1)} = 0. \qquad (64)$$

Evaluating (63) at the surface using (62), we find that

$$\mathrm{Im}\left\{\pi_s^{(1)}\right\} = c\ \mathrm{Im}\left\{\dot{\phi}_s^{(1)}\right\} , \qquad (65)$$

where the imaginary part of the phase speed may be

neglected since it is proportional to the wave growth. We may eliminate $\pi^{(1)}$ between (63) and (64) to obtain

$$\ddot{\phi}^{(1)} - k^2\phi^{(1)} = \frac{\ddot{U}}{U-c}\phi^{(1)}. \qquad (66)$$

Multiplying this equation by the complex conjugate ϕ^* and integrating from the surface to infinity, we obtain

$$\int_s^\infty \phi^*\ddot{\phi} - \int_s^\infty k^2\phi^*\phi = \int_s^\infty \frac{\ddot{U}}{U-c}\phi^*\phi. \qquad (67)$$

This proceedure produces the total energy per unit mass in the flow and is called the energy integral. The term on the left-hand side may be integrated by parts to obtain

$$-\int_s^\infty \dot{\phi}^*\dot{\phi} - \phi_s^*\dot{\phi}_s - \int_s^\infty k^2\phi^*\phi = \int_s^\infty \frac{\ddot{U}}{U-c}\phi^*\phi. \qquad (68)$$

Using the boundary conditions (62) and rearranging we have

$$-\frac{c}{k}\dot{\phi}_s^{(1)} = \int_s^\infty \left[|\dot{\phi}^{(1)}|^2 + k^2|\phi^{(1)}|^2 \right] + \int_s^\infty \frac{\ddot{U}}{U-c}|\phi^{(1)}|^2. \qquad (69)$$

The imaginary part of this expression is

$$\mathrm{Im}\left\{\pi_s^{(1)}\right\} = -k\,\mathrm{Im}\left\{\int_s^\infty \frac{\ddot{U}}{U-c}\,|\phi^{(1)}|^2\,dy\right\}, \quad (70)$$

and may be evaluated as a Cauchy Principle Value (c.f. Lin(1955) ch. 8).

Since a similar Cauchy principal value will be evaluated later, it is convenient to discuss the integration at this time for a general case. Let

$$I = \mathrm{Im}\left\{\int_s^\infty \frac{F(y)\,dy}{U-c}\right\}, \quad (71)$$

where F is regular and non-zero at U=c and where the imaginary part of c is taken as infinitesimally small and positive. The path of integration is along the U real axis, from values less than c_R to values greater than c_R. The pole of the integrand is then simple and lies in the upper-half U-plane, being arbitrarily close to $U=c_R$. For U monotone in y in the neighborhood of the pole, we may make U the independent variable and write

$$I = \mathrm{Im}\left\{\int_{U(s)}^{U(\infty)} \frac{F(y(U))}{U-c}\,\frac{dU}{\dot{U}}\right\}. \quad (72)$$

In the limit as $c_I \downarrow 0^+$, the path of integration may be taken as indented below the pole as shown

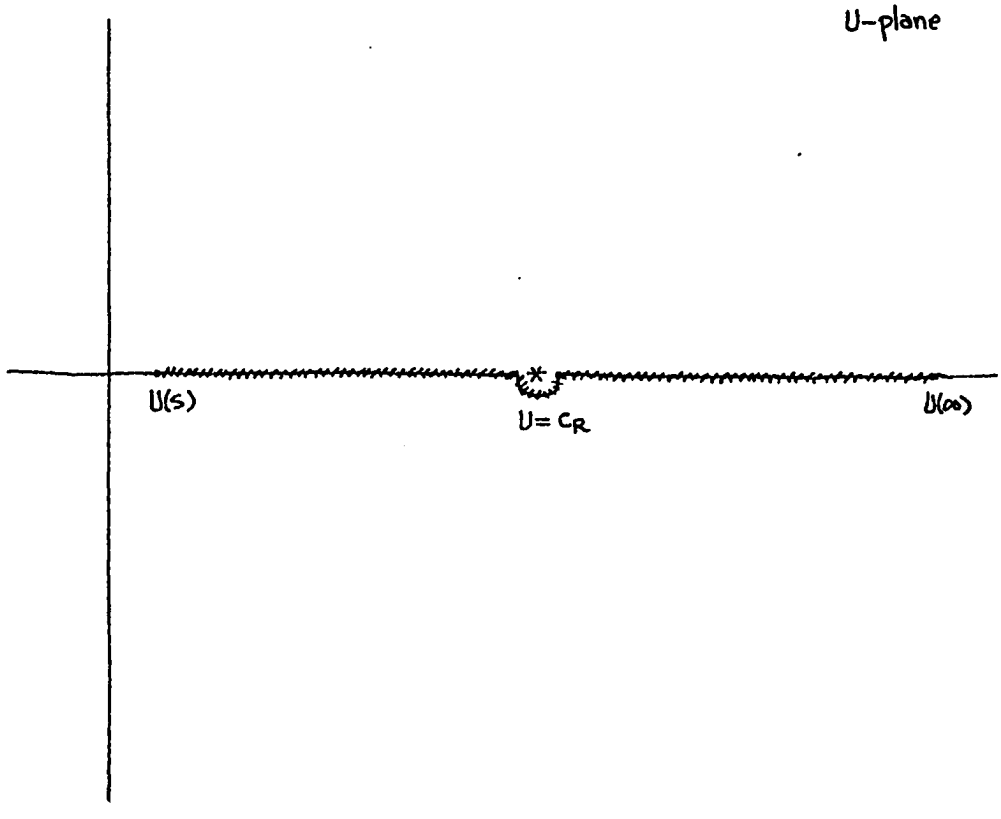

Figure 12. Path of integration in the complex U-plane required to evaluate (72). In the limit as c_I goes to 0+, the singularity approaches the path of integration. The path must then be indented below the singularity and the integral may be evaluated as a Cauchy Principal Value.

in Figure 12. The integral may then be evaluated as a Cauchy principal value, and, for example, using Hildebrand (1961) p557 theorem IV, we obtain

$$I = \mathrm{Im}\left\{ \pi i \ \mathrm{Residue}\left[\frac{F(y(U))}{\dot{U}} \right]_{U=c} \right\}. \qquad (73)$$

To lowest order in c_I, $U=c_R$ and we have

$$I = \frac{\pi}{\dot{U}_c} \mathrm{Re}\left\{ F(y_c) \right\}, \qquad (74)$$

where the subscript c indicates that the quantity is to be evaluated at the critical level, where $U=c_R$.

For the present case

$$F = -k \ddot{U} |\phi^{(1)}|^2, \qquad (75)$$

so that

$$\mathrm{Im}\left\{ \pi_s^{(1)} \right\} = -\pi k \frac{\ddot{U}_c}{\dot{U}_c} |\phi_c^{(1)}|^2. \qquad (76)$$

This is just Miles' (1957) "inviscid" result.

If $\ddot{U}_c=0$, as it is in the linear region, then it follows from (65) that $\mathrm{Im}\{\dot{\phi}_s^{(1)}\} = 0$. Since $\mathrm{Im}\{\phi_s^{(1)}\} = 0$ by (62) and since (66) is no longer

singular, then $Im\{\phi^{(1)}\} = 0$. We shall assume that this is the case (that $\ddot{U}_c=0$) and look for phase shifts which arise from perturbations to the turbulent stresses.

The $O(\epsilon_w \epsilon_T)$ equations are

$$(U-c)\dot{\phi}^{(2)} - \dot{U}\phi^{(2)} + \pi^{(2)} + \langle u^2\rangle^{(1)} + \frac{1}{ik}\langle \dot{uv}\rangle^{(1)} = 0 , \quad (77)$$

$$k^2(U-c)\phi^{(2)} + \dot{\pi}^{(2)} + ik\langle uv\rangle^{(1)} + \langle \dot{v}^2\rangle^{(1)} = 0. \quad (78)$$

Equation (77) evaluated on the surface, assuming that the water is not turbulent so that the turbulent perturbations vanish, becomes

$$\pi_s^{(2)} = \dot{U}_s \phi_s^{(2)} + c\dot{\phi}_s^{(2)} . \quad (79)$$

The imaginary part of this expression is

$$Im\{\pi_s^{(2)}\} = c\, Im\{\dot{\phi}_s^{(2)}\} . \quad (80)$$

Proceeding as before, we eliminate the pressure between (77) and (78) to obtain

$$(U-c)(\ddot{\phi}^{(2)} - k^2\phi^{(2)}) = \ddot{U}\phi^{(2)} - \langle \dot{u}^2\rangle^{(1)} + \langle \dot{v}^2\rangle^{(1)} - \frac{1}{ik}\left[\langle \ddot{uv}\rangle^{(1)} + k^2\langle uv\rangle\right]. \quad (81)$$

We may simplify this expression by using $\langle v^2\rangle \ll \langle u^2\rangle$ and $\frac{d^2}{dx^2} \ll \frac{d^2}{dy^2}$ to

$$\ddot{\phi}^{(2)} - k^2\phi^{(2)} = -\frac{\langle \dot{u}^2\rangle^{(1)} + \frac{1}{ik}\langle \ddot{uv}\rangle^{(1)} - \ddot{U}\phi^{(2)}}{U-c}. \quad (82)$$

We form the energy integral to order $\epsilon_W\epsilon_T$ by adding (66) to ϵ_T times (82), multiplying by $(\phi^{(1)}+\epsilon_T\phi^{(2)})^*$, and integrating from the surface to infinity. The result is

$$\int_s^\infty (\phi^{(1)}+\epsilon_T\phi^{(2)})^*(\phi^{(1)}+\epsilon_T\ddot{\phi}^{(2)}) - k^2\int_s^\infty |\phi^{(1)}+\epsilon_T\phi^{(2)}|^2 = -\int_s^\infty \frac{\langle \dot{u}^2\rangle^{(1)} + \frac{1}{ik}\langle \ddot{uv}\rangle^{(1)} - \ddot{U}\phi^{(1)}}{U-c}(\phi^{(1)}+\epsilon_T\phi^{(1)}$$

(83)

Again, we integrate the left-hand side of the equation by parts, using the boundary conditions (42) and the boundedness of ϕ to obtain

$$-\frac{c}{k}\epsilon_T\dot{\phi}_s^{(2)} = \int_s^\infty\left[|\dot{\phi}^{(1)}+\epsilon_T\dot{\phi}^{(2)}|^2 + k^2|\phi^{(1)}+\epsilon_T\phi^{(2)}|^2\right] - \epsilon_T\int_s^\infty \frac{\langle \dot{u}^2\rangle^{(1)} + \frac{1}{ik}\langle \ddot{uv}\rangle^{(1)}}{U-c}(\phi^{(1)}+\epsilon_T\phi^{(2)})^*$$
$$+ \int_s^\infty \frac{\ddot{U}}{U-c}|\phi^{(1)}+\epsilon_T\phi^{(2)}|^2. \quad (84)$$

The imaginary part of this expression reduces to

$$\mathrm{Im}\{\pi_s^{(2)}\} = k\,\mathrm{Im}\left\{\int_s^\infty \frac{\langle \dot{u}^2\rangle^{(1)} + \frac{1}{ik}\langle \ddot{uv}\rangle^{(1)}}{U-c}\phi^{(1)}dy + \int_s^\infty \frac{\ddot{U}}{U-c}|\phi^{(1)}+\epsilon_T\phi^{(2)}|^2 dy\right\}, \quad (85)$$

using (80), the reality of $\phi^{(1)}$, and dropping terms $O(\epsilon_T)^2$. Just as in the case of the "inviscid" result, the integral is evaluated by contour

integration as a Cauchy principal value. Comparing with our general expression, we see that

$$F = \left[\langle \dot{u}^2 \rangle^{(1)} + \frac{1}{ik} \langle \ddot{uv} \rangle^{(1)} \right] \phi^{(1)} + \ddot{U} \left| \phi^{(1)} + \epsilon_T \phi^{(2)} \right|^2 . \quad (86)$$

Using the reality of $\phi^{(1)}$, we have

$$Re\{F_c\} = \phi_c^{(1)} Re\left\{ \langle \dot{u}^2 \rangle_c^{(1)} + \frac{1}{ik} \langle \ddot{uv} \rangle_c^{(1)} \right\} + \ddot{U}_c \left| \phi_c^{(1)} + \epsilon_T \phi_c^{(2)} \right|^2 , \quad (87)$$

which is further simplified by the condition $\ddot{U}=0$ to

$$Re\{F_c\} = \phi_c^{(1)} Re\left\{ \langle \dot{u}^2 \rangle_c^{(1)} \right\} + \frac{1}{k} \phi_c^{(1)} Im\left\{ \langle \ddot{uv} \rangle_c^{(1)} \right\} . \quad (88)$$

We finally obtain the result

$$Im\{\pi_s^{(2)}\} = \frac{\pi k \phi_c^{(1)}}{\ddot{U}_c} \left[Re\left\{ \langle \dot{u}^2 \rangle_c^{(1)} \right\} + \frac{1}{k} Im\left\{ \langle \ddot{uv} \rangle_c^{(1)} \right\} \right] . \quad (89)$$

This equation relates the perturbations to the mean turbulent Reynolds stresses at the critical level to the surface pressure in phase with the wave slope. This is the generalization of Miles' result to include wave-induce turbulence interactions. However, as opposed to the "inviscid" theory, it is necessary to consider additional interactions

to specify the turbulent stress perturbations. This is determined in the next section.

3.6 PERTURBATIONS TO THE TURBULENT STRESSES AT THE CRITICAL LEVEL CAUSED BY WAVE-INDUCED MOTIONS

As has been discussed by Lighthill (1962), the wave-induced flows near the critical level cause a closed-streamline region to develop, the critical layer. If a diffusive mechanism is present, this motion can cause the mechanical transport of fluid properties which have gradients in this region. We shall calculate the perturbations to the turbulent stresses which are caused by mixing in the critical layer.

Multiplying (57) by the fluctuating part of the velocity, u_k, and taking the ensemble average, we obtain

$$0 = \langle u_K \frac{\partial}{\partial t} u_i \rangle + \langle u_K \frac{\partial}{\partial x_j} [u_i u_j + \frac{1}{\rho_a} p \delta_{ij}] \rangle . \quad (90)$$

Using the vanishing of the mean of fluctuating parts, the non-zero part of the above expression is

$$0 = \langle u_K \frac{\partial}{\partial t} u_i \rangle + \langle u_K \frac{\partial}{\partial x_j} (U_i u_j) \rangle + \langle u_K \frac{\partial}{\partial x_j} (u_i U_j) \rangle + \langle u_K \frac{\partial}{\partial x_j} (u_i u_j) \rangle + \frac{1}{\rho_a} \langle u_K \frac{\partial}{\partial x_i} p \rangle . \quad (91)$$

Interchanging the free indicies i and K we obtain the equation

$$0 = \langle u_i \frac{\partial}{\partial t} u_K \rangle + \langle u_i \frac{\partial}{\partial x_j} U_K u_j \rangle + \langle u_i \frac{\partial}{\partial x_j} u_K U_j \rangle + \langle u_i \frac{\partial}{\partial x_j} u_K u_j \rangle + \frac{1}{\rho_a} \langle u_i \frac{\partial}{\partial x_K} p \rangle . \tag{92}$$

Adding the two forms and grouping together similar terms, we have

$$\begin{aligned} 0 = & \langle u_K \frac{\partial}{\partial t} u_i + u_i \frac{\partial}{\partial t} u_K \rangle + \langle u_K \frac{\partial}{\partial x_j} U_i u_j + u_i \frac{\partial}{\partial x_j} U_K u_j \rangle \\ & + \langle u_K \frac{\partial}{\partial x_j} u_i U_j + u_i \frac{\partial}{\partial x_j} u_K U_j \rangle + \langle u_K \frac{\partial}{\partial x_j} u_i u_j + u_i \frac{\partial}{\partial x_j} u_K u_j \rangle \\ & + \frac{1}{\rho_a} \langle u_K \frac{\partial}{\partial x_i} p + u_i \frac{\partial}{\partial x_j} p \rangle . \end{aligned} \tag{93}$$

A single time derivative $\frac{\partial}{\partial t}\langle u_i u_K \rangle$ may be formed from the first term. Expanding the second averaged quantity gives

$$u_K U_i \frac{\partial u_j}{\partial x_j} + u_K u_j \frac{\partial U_i}{\partial x_j} + u_i U_K \frac{\partial u_j}{\partial x_j} + u_i u_j \frac{\partial U_K}{\partial x_j} , \tag{94}$$

which, upon using the continuity equation for the fluctuating flow, $\frac{\partial u_j}{\partial x_j} = 0$, becomes

$$u_K u_j \frac{\partial U_i}{\partial x_j} + u_i u_j \frac{\partial U_K}{\partial x_j} \tag{95}$$

The third term when expanded is

$$u_K u_i \frac{\partial U_j}{\partial x_j} + u_K U_j \frac{\partial u_i}{\partial x_j} + u_i u_K \frac{\partial U_j}{\partial x_j} + u_i U_j \frac{\partial u_K}{\partial x_j} . \quad (96)$$

Using the continuity equation for the mean flow, $\frac{\partial U_j}{\partial x_j} = 0$, this becomes

$$u_K U_j \frac{\partial u_i}{\partial x_j} + u_i U_j \frac{\partial u_K}{\partial x_j} , \quad (97)$$

or

$$U_j \frac{\partial}{\partial x_j}(u_i u_K) . \quad (98)$$

The fourth term may be similarly reduced to

$$\frac{\partial}{\partial x_j}(u_i u_j u_K) , \quad (99)$$

so that the final form of the equation is

$$\frac{\partial}{\partial t}\langle u_i u_K\rangle + U_j \frac{\partial}{\partial x_j}\langle u_i u_K\rangle = -\left[\langle u_i u_K\rangle \frac{\partial U_j}{\partial x_K} + \langle u_j u_K\rangle \frac{\partial U_i}{\partial x_K}\right] - \left\langle u_i \frac{\partial p}{\partial x_j} + u_j \frac{\partial p}{\partial x_i}\right\rangle - \frac{\partial}{\partial x_K}\langle u_i u_j u_K\rangle , \quad (100)$$

(c.f. Townsend (1956) p.26). These terms can be interpreted as the stress balance between the advection by the mean flow, the production from the mean flow, the loss to turbulent pressure forces, and the diffusion by turbulent mixing.

As has been pointed out earlier, this second-order moment equation contains third-order moments whose values must be specified to make the problem determinant. From our physical reasoning, it is the diffusive aspects of turbulence which will be important in the neighborhood of the critical layer. We therefore employ a closure hypothesis which makes explicit the mixing effects of turbulent flows: the equivalent eddy diffusion. According to this assumption we may write

$$\langle u_i u_j u_k \rangle = - \nu_E \frac{\partial}{\partial x_k} \langle u_i u_j \rangle \,, \qquad (101)$$

where ν_E is the eddy diffusion coefficient determined from the momentum flux as discussed in section 2.

Using (61) the $O(\epsilon_T)$ equations are

$$-\langle uv \rangle^{(0)} \dot{U} = \left\langle u \frac{\partial p}{\partial x} \right\rangle^{(0)}, \qquad (102)$$

$$-\langle v^2 \rangle^{(0)} \dot{U} = \left\langle u \frac{\partial p}{\partial y} + v \frac{\partial p}{\partial x} \right\rangle^{(0)}, \qquad (103)$$

which express the balance between production from

the mean flow by vertical fluctuations and the transfer tothe water by pressure forces.

The $O(\epsilon_T \epsilon_W)$ equations are

$$\nu_E \langle \ddot{u^2} \rangle^{(1)} - ik(U-c)\langle u^2 \rangle^{(1)} + ik\phi^{(1)}\langle \dot{u^2} \rangle^{(0)} = 2\langle u \frac{\partial p}{\partial x} \rangle^{(1)} + 2\left\{ ik\langle u^2 \rangle^{(0)} \dot{\phi}^{(1)} + \langle uv \rangle^{(0)} \ddot{\phi}^{(1)} + \langle uv \rangle^{(1)} \dot{U} \right\}, \tag{104}$$

and

$$\nu_E \langle \ddot{uv} \rangle^{(1)} - ik(U-c)\langle uv \rangle^{(1)} + ik\phi^{(1)}\langle \dot{uv} \rangle^{(0)} = \langle u \frac{\partial p}{\partial y} + v \frac{\partial p}{\partial x} \rangle^{(1)} + \left\{ \langle u^2 \rangle^{(0)} k^2 \phi^{(1)} + \langle v^2 \rangle^{(1)} \dot{U} \right\}. \tag{105}$$

We specifically wish to consider the perturbations which arise because of mixing effects in the critical layer. From our physical model, and by analogy with the $O(\epsilon_T)$ equations, we expect any stress production from the mean flow to be transferred to the water by pressure forces. Therefore, the perturbation to the pressure work terms should just balance the perturbations to the production terms (enclosed in braces). The $O(\epsilon_T \epsilon_W)$ equations are then

$$\nu_E \langle \ddot{u^2} \rangle^{(1)} - ik(U-c)\langle u^2 \rangle^{(1)} = -ik\phi^{(1)}\langle \dot{u^2} \rangle^{(0)}, \tag{106}$$

$$\nu_E \langle \ddot{uv} \rangle^{(1)} - ik(U-c)\langle uv \rangle^{(1)} = -ik\phi^{(1)}\langle \dot{uv} \rangle^{(0)}. \tag{107}$$

The perturbations are now only driven by the terms which represent mixing of the critical layer, that is, due to advection by the wave-induced flow.

Since the thickness of the critical layer is small compared with the distance over which the mean flow quantities change appreciably and since $\phi^{(1)}$ varies over a distance of k^{-1} which is also large compared with the critical layer, we may treat the right-hand sides of (106) and (107) as constant and equal to their values at the critical level. Both equations then have the form

$$\nu_E \ddot{Q} - ik\dot{U}(y-y_c)Q = -ik\phi_c^{(1)}\dot{Q}_c^{(0)} \quad , \tag{108}$$

where we have used the expression for U valid near the critical level. We make the following change of variables

$$y-y_c = \left(\frac{\nu_E}{ik\dot{U}}\right)^{1/3} z \quad , \quad Q = \frac{1}{\nu_E}\left(\frac{\nu_E}{ik\dot{U}}\right)^{2/3}\left(-ik\phi_c^{(1)}\dot{Q}_c^{(0)}\right)\tilde{Q} \, , \tag{109}$$

which reduces (108) to the form

$$\frac{d^2\tilde{Q}}{dz^2} - z\tilde{Q} = 1. \tag{110}$$

The general solution of this equation is

$$\tilde{Q} = a\,Ai(z) + b\,Bi(z) + \pi \int_0^z [Ai(x)Bi(z) - Ai(z)Bi(x)]\,dx, \tag{111}$$

where Ai and Bi are the Airy functions of the first and second kind, respectively, defined by

$$Ai(z) = \frac{1}{\pi} \int_0^\infty \cos\left(\tfrac{1}{3}t^3 + zt\right) dt, \tag{112}$$

$$Bi(z) = \frac{1}{\pi} \int_0^\infty \left[e^{-\frac{1}{3}t^3 + zt} + \sin\left(\tfrac{1}{3}t^3 + zt\right) \right] dt. \tag{113}$$

The conditions on Q are that it must be bounded at large distances above the critical level and vanish at the water surface. We first consider the restrictions placed on a and b by the condition of boundedness as $y \to \infty$, or $z \to \infty\, e^{\pi i/6}$.

We may rewrite (111) as

$$\tilde{Q} = aAi(z) + bBi(z) + \pi Bi(z) \int_0^{\infty e^{\pi i/6}} Ai(x)dx - \pi Bi(z) \int_z^{\infty e^{\pi i/6}} Ai(x)dx - \pi Ai(z) \int_0^{z_0} Bi(x)dx - \pi Ai(z) \int_{z_0}^{z} Bi(x)d \tag{114}$$

where z_0 is a large, fixed number chosen so that the asymptotic forms used below will be accurate for $z > z_0$ to a predetermined desired accuracy. From Abramowitz and Segun (1956), hereafter abbreviated A&S, we find the asymptotic formulae

$$Ai(z) \sim \tfrac{1}{2}\pi^{-1/2} z^{-1/4} e^{-\frac{2}{3}z^{3/2}}, \qquad (115)$$

$$Bi(z) \sim \pi^{-1/2} z^{-1/4} e^{+\frac{2}{3}z^{3/2}}, \qquad (116)$$

valid for $z \to +\infty e^{\pi i/6}$. Using these in the fourth and sixth terms of (114) and integrating by parts, we obtain

$$\tilde{Q} = \left[a - \pi \int_0^{z_0} Bi(x)\,dx\right] Ai(z) + \left[b + \pi \int_0^{\infty e^{\pi i/6}} Ai(x)\,dx\right] Bi(z) - \frac{1}{z}. \qquad (117)$$

The second term grows with z, so that boundedness requires the choice

$$b = -\pi \int_0^{\infty e^{\pi i/6}} Ai(x)\,dx \qquad (118)$$

$$= -\pi/3, \qquad (119)$$

where the latter results follows from the contour integration along the path shown in Figure 13 and the formula from A&S

$$\int_0^{\infty} Ai(x)\,dx = \tfrac{1}{3}. \qquad (120)$$

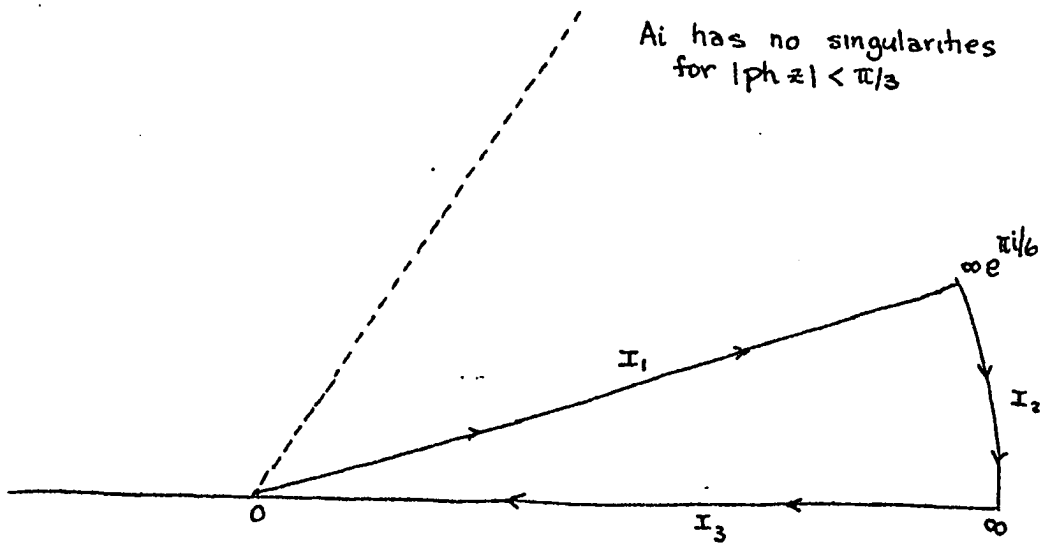

$$I_1 + I_2 + I_3 = 0$$

$$I_2 = 0$$

$$\int_0^{\infty e^{\pi i/6}} Ai(z)\,dz = -\int_\infty^0 Ai(z)\,dz$$

$$= \int_0^\infty Ai(z)\,dz$$

Figure 13. Contour integration in the complex z-plane.

$\underline{a}$ is determined by the condition that the perturbations vanish on the water surface. This makes $\underline{a}$, in general, dependent on the aerodynamic and wave parameters. If, however, the critical layer is well-separated from the boundary, that is, the distance from the mean water level to the critical level is much larger than the critical layer thickness, then z takes on a large value at the surface and $\underline{a}$ may be determined by the asymptotic form. We therefore choose $\underline{a}$ so that the solution vanishes as $z \to -\infty e^{\pi i/6}$. Let $z = -\eta$, then from A&S we find the proper asymptotic formulae to be

$$\begin{aligned} Ai(z) = Ai(-\eta) &\cong \pi^{-1/2}\eta^{-1/4} \sin\left(\tfrac{2}{3}\eta^{3/2} + \tfrac{\pi}{4}\right), \\ &= \tfrac{1}{2i}\pi^{-1/2}\eta^{-1/4}\left[e^{i\left(\frac{2}{3}\eta^{3/2} + \frac{\pi}{4}\right)} - e^{-i\left(\frac{2}{3}\eta^{3/2} + \frac{\pi}{4}\right)}\right] \\ &\sim iF \end{aligned} \tag{121}$$

where $F = \tfrac{1}{2}\pi^{-1/2}\eta^{-1/4} e^{-i\frac{2}{3}\eta^{3/2}} e^{-\pi i/4}$, the dominant exponential as $\eta \to +\infty e^{\pi i/6}$. Similarly, one finds.

$$Bi(z) = Bi(-\eta) \sim F. \tag{122}$$

Equation ( ) then takes on the form

$$\tilde{Q} = a\,Ai(-\eta) - \frac{\pi}{3} Bi(-\eta) + \pi \int_0^{-\eta} [Ai(x)\,Bi(-\eta) - Bi(x)\,Ai(-\eta)]\,dx ,$$

$$= \left\{ ia - \frac{\pi}{3} + \pi \int_0^{-\eta} [Ai(x) - i\,Bi(x)]\,dx \right\} F ,$$

$$= \left\{ ia - \frac{\pi}{3} + 2\pi e^{-\pi i/3} \int_0^{-\eta} Ai(x\,e^{2\pi i/3})\,dx \right\} F , \tag{123}$$

where the last form results from using the identity

$$Ai(x) - i\,Bi(x) = 2\,e^{-\pi i/3}\,Ai(x\,e^{2\pi i/3}). \tag{124}$$

Introducing the new variable $x = -\xi e^{\pi i/6}$ (which takes on only real values for the integration of interest), we find

$$\int_0^{-\eta} Ai(x e^{2\pi i/3})\,dx = \int_0^{\infty} Ai(-\xi\,e^{\pi i/6} e^{2\pi i/3})\;(-d\xi\,e^{\pi i/6}),$$

$$= -\,e^{\pi i/6} \int_0^{\infty} Ai(\xi\,e^{\pi i/6})\,d\xi , \tag{126}$$

$$= -\tfrac{1}{3} e^{\pi i/6},$$

where the last result, as before, proceeds from

contour integration and the use of (120). Since F is unbounded as $\eta \to \infty e^{\pi i/6}$, $\underline{a}$ must be chosen so that the quantity within the braces vanishes. The solution is not only bounded, but vanishes, as required, at the water surface. This leads to

$$a = -\frac{\pi}{3}\left[1 + i(1+\sqrt{3})\right]. \tag{127}$$

Returning to the original variables, we may evaluate the perturbations to the turbulent stresses at the critical level. We find

$$\mathrm{Re}\left\{ \langle \dot{u}^2 \rangle_c^{(1)} \right\} = \frac{\pi C_2}{3}(1+\sqrt{3})\,\frac{1}{\nu_E}\left(\frac{\nu_E}{k\dot{U}}\right)^{1/3} k\phi_c^{(1)} \langle \dot{u}^2 \rangle_c^{(0)}, \tag{128}$$

$$\frac{1}{k}\,\mathrm{Im}\left\{ \langle \ddot{uv} \rangle_c^{(1)} \right\} = -\frac{\phi_c^{(1)}}{\nu_E} \langle \dot{uv} \rangle_c^{(0)}, \tag{129}$$

where $c_2 = -\mathrm{Ai}(0) = .25881\ldots$. Equation (89) may then be evaluated and yields

$$\tau/s = \frac{\pi k \left[\phi_c^{(1)}\right]^2}{c^2}\left[-\frac{\langle \dot{uv} \rangle_c^{(0)}}{u_*^2} + \frac{\pi C_2 (1+\sqrt{3})}{3}\left(\frac{k u_*}{\dot{U}_c}\right)^{2/3} \frac{\langle \dot{u}^2 \rangle_c^{(0)}}{u_*^2} \right], \tag{130}$$

where equation (3) has been used to eliminate the eddy diffusion coefficient.

This equation relates the wave growth of the surface wave to the initial gradients in the mean turbulent stresses and to the properties of the wave-induced flow. This result has been obtained without recourse to approximation, although, of course, certain assumptions concerning the nature of the flow was made initially. However, the formula (130) contains the quantity $\phi_c^{(1)}$, which requires solution of the $O(\epsilon_w)$ equations for the specific velocity profile U(y). In the next section we shall develop an approximate solution which allows $\phi_c^{(1)}$ to be determined with sufficient accuracy for our present needs.

3.7 APPROXIMATE SOLUTION TO THE MAGNITUDE OF THE WAVE-INDUCED FLOW AT THE CRITICAL LEVEL

Following Miles (1957), we multiply (66) by (U-c) and integrate from the critical level to infinity to obtain

$$\phi_c^{(1)} = \frac{1}{U_c} \int_{y_c}^{\infty} k^2 (U-c) \phi^{(1)} \, dy . \qquad (131)$$

The smoothing effects of integration allow an approximate form of $\phi^{(1)}$ to be used on the right-hand side of this equation. Since the integrand vanishes near the critical level, the trial solution need not be accurate in this region. Conte and Miles (1959) have discussed this point thoroughly and have shown that this technique is insensitive to errors, even when the correct solution possesses a logarithmic singularity at the critical level.

Inspired by the unsheared solution of Kelvin, Miles proposed the trial solution

$$\phi^{(1)} = (U-c) \frac{e^{-ky}}{k} \qquad (132)$$

This solution may be physically interpreted that the primary effect of the surface wave is to cause

the flow to bend around the wavy surface. Benjamin has shown that this is the dominant effect on the airflow everywhere above the critical level.

If $\phi_c^{(1)}$ is written in the dimensionless form

$$\phi_c^{(1)} = \frac{c^2}{U_c} \alpha_c , \tag{133}$$

Miles' approximation leads to

$$\alpha_c = \int_{y_c}^{\infty} \left(\frac{U}{c}-1\right)^2 e^{-ky}\, k\,dy. \tag{134}$$

For the particular velocity profile

$$U = \begin{cases} U_K (y/k_s) & y \le k_s \\ U_K + U_1 \ln (y/k_s) & y \ge k_s \end{cases} , \tag{135}$$

where U_k is the velocity at $y=k_s$. By direct substitution we obtain

$$\alpha_c \equiv I_1 + I_2 = \int_{y_c}^{k_s} \left(\frac{U_K}{c}\frac{y}{k_s}-1\right)^2 e^{-ky} k\,dy + \int_{k_s}^{\infty} \left(\frac{U_K + U_1 \ln (y/k_s)}{c} - 1\right)^2 e^{-ky}\, k\,dy. \tag{136}$$

In I_1, let $\xi = \frac{U_K}{c}\frac{y}{k_s} - 1$, then

$$I_1 = De^{-D} \int_0^B \xi^2 e^{-D\xi} d\xi , \tag{137}$$

where $B = \frac{v_k}{c} - 1$ and $D = \frac{kk_s c}{v_k}$. By elementary integration, we find

$$I_1 = \frac{2e^{-D}}{D^2}\left[1 - e^{-DB}(1 + DB + \tfrac{1}{2}D^2B^2)\right]. \quad (138)$$

In I_2, let $\xi = \frac{y}{k_s} e^{B/A}$, where $A = v_1/c$, then

$$I_2 = \int_{e^{B/A}}^{\infty} A^2 \ln^2\xi \, e^{-\mu\xi} \, \mu d\xi, \quad (139)$$

where $\mu = kk_s e^{-B/A}$. We then write

$$I_2 = \left\{ \int_0^{\infty} - \int_0^{e^{B/A}} \right\} A^2 \ln^2\xi \, e^{-\mu\xi} \, \mu d\xi \equiv I_3 - I_4 . \quad (140)$$

I_3 may be evaluated directly, see Gradshteyn and Ryzhik (1969) formula 4.335 1, to give

$$I_3 = A^2\left[\frac{\pi^2}{6} + \ln^2 C\mu\right] \quad (141)$$

where C = Euler's constant, 1.78... . Using the definition of μ , we obtain

$$I_3 = \frac{\pi^2 A^2}{6} + \left[A \ln C k k_s - B\right]^2. \quad (142)$$

I_4 may be evaluated most easily by expanding the exponential as a power series and integrating term by term.

$$I_4 = \int_0^{e^{B/A}} A^2 \ln^2\xi \, e^{-\mu\xi} \, \mu \, d\xi \,, \tag{143}$$

$$= A^2\mu \int_0^{e^{B/A}} \ln^2\xi \sum_{m=0}^{\infty} \frac{(-\mu\xi)^m}{m!} \, d\xi \,, \tag{144}$$

$$= A^2 \sum_{m=0}^{\infty} \frac{(-1)^m \mu^{m+1}}{m!} \int_0^{e^{B/A}} \xi^m \ln^2\xi \, d\xi \,. \tag{145}$$

Using G&R formula 2.723 2, we obtain

$$I_4 = -A^2 \sum_{m=0}^{\infty} \frac{(-\mu\xi)^{m+1}}{(m+1)!} \left[\ln^2\xi - \frac{2\ln\xi}{m+1} + \frac{2}{(m+1)^2} \right]_0^{e^{B/A}} , \tag{146}$$

which reduces to

$$I_4 = -\sum_{m=0}^{\infty} \frac{(-1)^{m+1}}{(m+1)!} (kk_s)^{m+1} \left[B^2 - \frac{2AB}{m+1} + \frac{2A^2}{(m+1)^2} \right] . \tag{147}$$

Combining (138), (140), (142), and (147) we have

$$\alpha_c = \frac{\pi^2 A^2}{6} + \left[A \ln(kk_s) - B \right]^2 + \sum_{m=0}^{\infty} \frac{(-kk_s)^{m+1}}{(m+1)!} \left[B^2 - \frac{2AB}{m+1} + \frac{2A^2}{(m+1)^2} \right]$$

$$+ \frac{2e^{-D}}{D^2} \left[1 - e^{-BD} \left(1 + BD + \tfrac{1}{2} B^2 D^2 \right) \right] . \tag{148}$$

Equation (139) and the expression for the wave-induced flow, equation (148), determine the rate of growth of an infinitesimal surface disturbance. Since the growth rate is proportional to the gradient at the critical level, we can say that the most unstable mode, that is, the mode which will be first observed, is the mode whose phase speed is equal to the mean horizontal velocity at the height where the turbulent gradient is largest. In section 4 we shall specialize these results to the case of ocean wave growth.

3.8 SUMMARY

This this section we examined the stability of turbulent flows in the presence of a flexible boundary. The effects of turbulence was taken into account by considering that it is a perturbation of the wave-induced flow. It was shown that the pressure at the boundary in phase with the wave slope was determined soley in terms of fluid properties at the critical level. The diffusive nature of turbulent flows was emphasized by employing an eddy diffusion along gradients to close the turbulence equations of motion. The wave-induced flow at the critical level was shown to cause large changes in the mean turbulent stresses there and lead to a surface pressure distribution which causes the wave to grow. Finally, approximate values of the wave-induced flow were derived, allowing the growth rate of the disturbance to be expressed in terms of the initial flow parameters.

4. A THEORY OF OCEAN WAVE GENERATION

4.1 THE FORMULAE

In the preceeding sections, we derived expressions for the mean airflow near water waves and the growth rates of small surface perturbations in terms of mean airflow quantities. From section 2 we have the following forms for the mean horizontal velocity and the mean turbulent Reynolds stresses

$$U = U_K \, (y/k_s), \tag{149}$$

$$\langle uv \rangle^{(0)} = (\tau_w/\tau) \, u_*^2 \, (y/k_s), \tag{150}$$

$$\langle u^2 \rangle^{(0)} = \gamma \, u_*^2 \, (y/k_s), \tag{151}$$

where U_k is the value of the air velocity at k_s, τ_w is the wave drag, τ is the total momentum flux to the water, $u_* = (\tau / \rho_a)^{1/2}$ is the shear velocity, γ is the dimensionless turbulence intensity at the edge of the linear region, and

$k_s = 2\sqrt{2}\,\sigma$ is the average waveheight.

Using these expressions in (130) and simplifing, we have

$$\varsigma/_S = \pi g \frac{k_s \alpha_c^2}{U_K^2}\left[(\tau_w/\tau) + \frac{\pi C_2(1+\sqrt{3})}{3}\gamma\left(\frac{K k_s u_*}{U_K}\right)^{2/3}\right]. \quad (152)$$

This equation, and (148) giving the wave-induced pressure at the critical layer

$$\alpha_c = \frac{\pi^2 A}{6} + [A \ln C k k_s - B]^2 + \sum_{m=0}^{\infty} \frac{(-k k_s)^{m+1}}{(m+1)!}\left[B^2 - \frac{2AB}{m+1} + \frac{2A^2}{(m+1)^2}\right] + \frac{2e^{-D}}{D^2}\left[1 - e^{-BD}\left(1 + BD + \tfrac{1}{2}B^2D^2\right)\right], \quad (153)$$

quoted here for reference, determine the wave growth in terms of the parameters of the airflow and the wave spectrum.

4.2 PHYSICAL INTERPRETATION

The goal of this work has been to study ocean wave generation with a maximum of physical insight and a minimum of empiricism. It is therefore appropriate to interpret our final result in terms of a physical argument which describes the mechanism whereby energy is transferred to the growing wave.

We return to the instantaneous airflow over a large wave, neglecting for the moment the growing wave. Fluid particles in the free stream have large horizontal velocities and small vertical velocities, which are of the order of the vertical fluctuations. Within the wake, on the other hand, the horizontal and vertical velocities are small and of the same order, because the streamlines are closed and the wave height and lengths are about the same size. This is schematically illustrated in Figure 14 .

Wave drag may be understood as follows. When fluid particles in the free stream and near the separation streamline cross the streamline because of vertical fluctuations (turbulence), they give up most of their horizontal momentum and energy

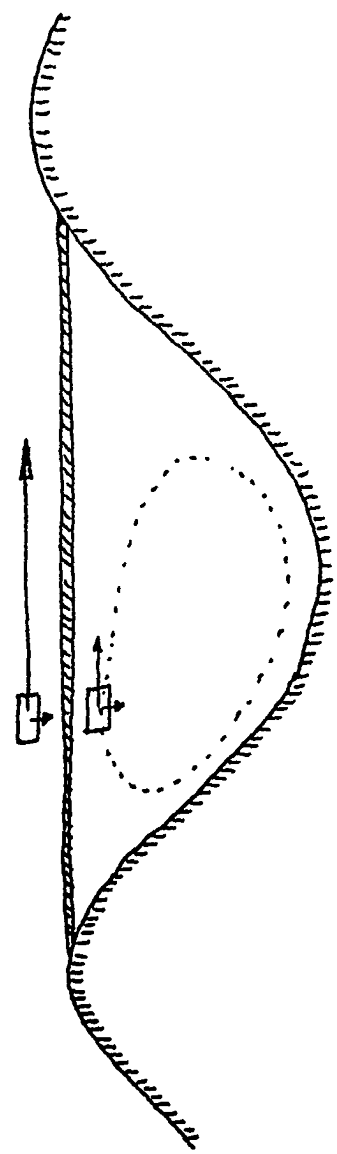

Figure [illegible]. Illustrates that the momentum at the pressure [illegible] at the separation streamline is just such as to produce the circulating motion of the water.

to the separation pressure forces. Once in the wake, their horizontal and vertical velocities are more nearly equal and they take part in the circulating motion there. See Figure 14. This loss of free stream momentum is seen as wave drag when the flow is averaged.

Now consider the perturbations caused by a small wave. The high pressures, which always develop in the flow above a wave crest, slow down the mean airflow there and force a downward motion ahead of the crest. On the average, this causes fluid particles to cross the separation streamline more often ahead of the crest of the growing wave than behind. This systematic loss of energy from the mean flow causes a pressure distribution to form which does work on the growing wave, just as in the "inviscid" theory.

It is important to note the difference between these ideas and those of Jeffreys (1925). Jeffreys assumed that separation occurred at the crest of the growing wave. This will not occur because the growing wave is too smooth ($ka \ll 1$) and because the relative velocity of the air will be too small (the waves have phase speeds greater than Wu's criterion, say). The present theory shows that

it is the separation from the slow ripples, riding atop the large waves in the spectrum, which is subtley modified by the critical layer of the growing wave and produces the energy transfer.

4.3 COMPARISON WITH OTHER GENERATION THEORIES

In the previous section we discussed the connection of the present theory with Jeffreys' use of separation. An actual comparison can only be made on the basis of numerical predictions of wave growth. In this respect other generation theories may be divided into two classes: those which involve no free parameters not determined by direct measurement, the only example being the "inviscid" theory, and those which have undetermined parameters, which are all the rest. We first consider Miles' theory, which we found to be a special case of the present theory.

The model of the mean airflow developed in section 2 shows that the velocity profile curvature in the linear region is zero or very small. Miles' theory would predict no wave growth and there is no comparison. However, if the velocity profile assumed by Miles (1959) did apply, the "inviscid" theory would predict the growth rates shown in Figure 15. The circles in this figure are the data of Dobson's (1971) run 4a, the most favorable case for Miles' theory. The "inviscid" theory is simply not correct. Also shown is the

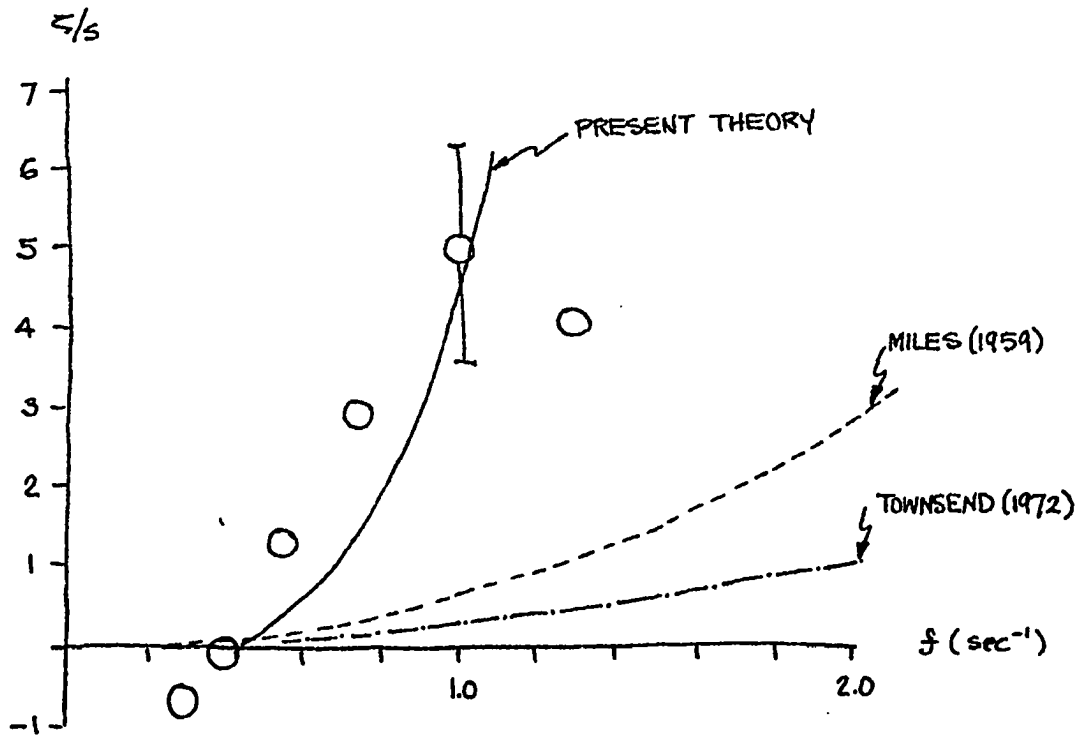

Figure 15. Comparison of the predictions of the present theory and those of Miles' "inviscid" theory (1959) and a recently reported numerical intergation of the turbulence equations by Townsend (1972). The data points are from Dobson (1971) run #4a, the run most favorable to Miles' theory.

recently reported predictions of numerical integrations of a turbulence theroy of Townsend (1972). This theory, although containing free constants, chooses those constants on the basis of completely independent experiments and so is less liable to the bias of forcing a "best fit". The result is even in greater disagreement with experiment than Miles' theory.

All other theories, with the exception of the present one and that of Longuet-Higgins (1969), make the initial assumption that the other waves have no influence on the mean airflow or water motions. This means that the growth rates are determined strictly in terms of the wind velocity, independently of the sea conditions. In fact, these theories predict growth rates which are functions only of the wave age, the ratio of the wave phase speed and the wind velocity. Dobson's data clearly indicates that the growth rates can vary by a factor of three at high wind speeds for a constant wave age. See Figure 16. Thus, not only are these theories arbitrary in that they contain parameters which can be adjusted without restriction, but their basic physical assumptions will not allow them to reproduce the

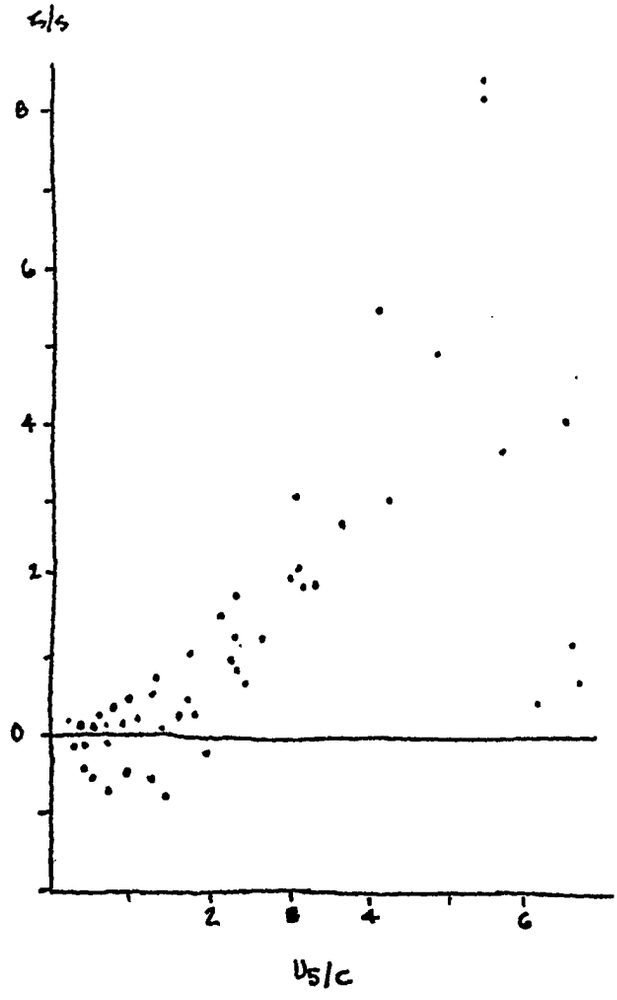

Figure 16. Plot of wave growth versus wave age using all of the data of all of the runs of Dobson (1971). The scatter shows that the wave growth is <u>not</u> a function of the wave age only.

important variations actually observed in field measurements.

A theory which does attempt to model the actual sea conditions, and which perhaps complements the present theory at longwavelengths, is that of Longuet-Higgins (1969). His arguments are completely heuristic, hence do not lead to numerical predictions, but are physically reasonable and probably, to some extent, occur in the ocean.

Consider a long wavelength, large amplitude wave. Figure 17a shows the actual motion of the water particles at the crest and trough of a gravity wave. The particles are in nearly circular motion, moving in the same direction as the wave as the crest passes and in the opposite direction at the trough. The velocity of the water particles are much slower than the phase speed of the waveform, being of the order of (ka) smaller. Thus even for the low-frequency, long-wavelength, high phase speed waves, the water velocity remains small.

For large amplitude waves, the waveform can become too steep to support the motion and the wave "breaks". Water is thrown forward from the crest of the wave and lands on the leeward face.

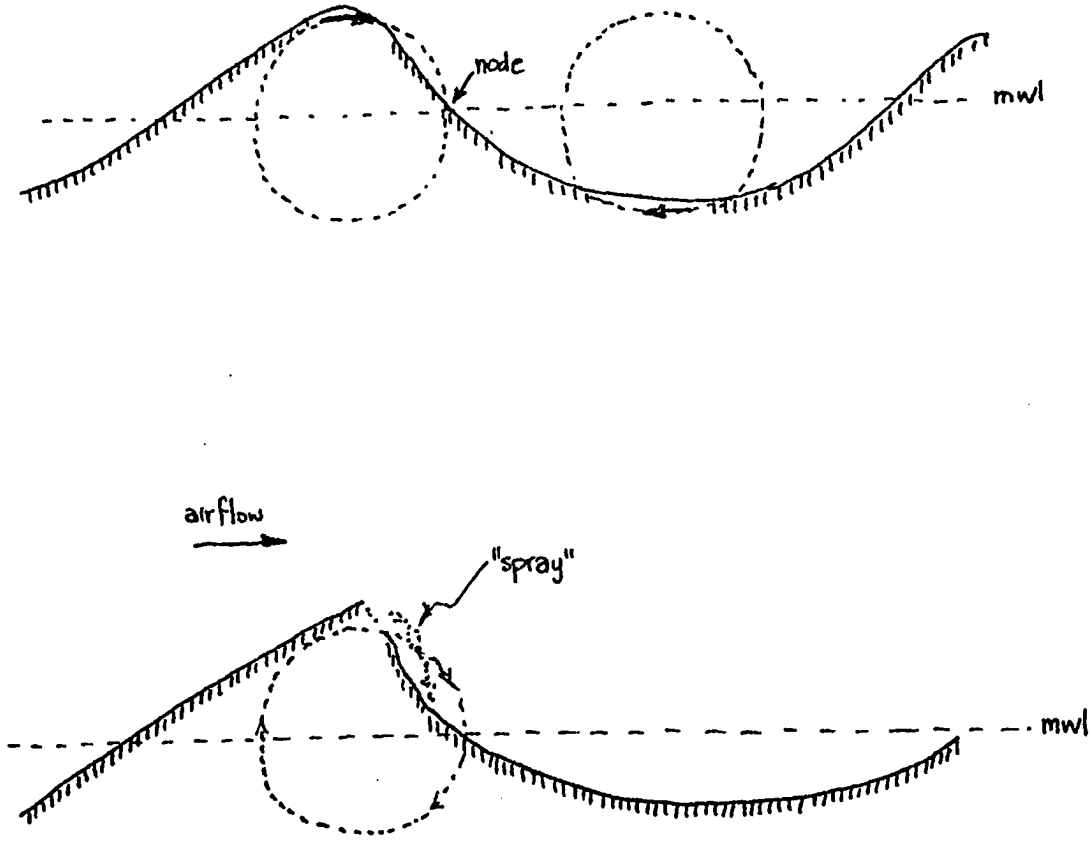

Figure 17. Illustration of the "spray" mechanism of Longuet-Higgins (1969). The upper diagram indicates the motion of the water particles in a progressing surface wave: they move with the wave as the crest passes, against it as the trough passes. The lower diagram indicates the "spray" blown off of the crest of a breaking wave. If the free water particles strike the wave before the node, momentum will be imparted to the orbital motion, causing the wave to grow.

If it strikes the surface before the node, the momentum will tend to increase the orbital motion of the water particles, thus causing the wave to grow. Since the orbital motion is always small, growth can occur even at relatively small wind speeds. We shall see that wave influences at small wind speeds also occur in the present theory.

This "spray" mechanism of Longuet-Higgins is limited to larger waves for two reasons. Firstly, as with separation, only the biggest waves, those which 'stand out' from the surface, will have the opportunity to have breaking regularly occur at their crests. The small waves, even if very steep, will spend most of the time far below the crests of the larger waves and will be sheltered from the winds which drive the breaking process. Secondly, it is very critical that the spray strikes the wave before the node. Otherwise, the momentum transfer opposes the orbital motion and the effect is cancelled out or the wave is actually beaten down. Since the distance travelled by the spray is scaled by the largest waves, those waves which are considerably shorter will feel no net effect.

As we shall see in the detailed comparison with the data of Dobson, the present separation

theory fails to predict the energy transfer to the large dominant waves. It is possible that the "spray" theory is just the complementing process at these long wavelengths. However, since the theory has no rigorous mathematical basis, quantitative assessment is not possible.

4.4 COMPARISON WITH EXPERIMENT

The most extensive data yet taken of wind-generated wave growth were made by Dobson (1971) in the Burrard Inlet near Vancouver. These involved the simultaneous measurement, by a vertically constrained bouy, of the water surface displacement and the aerodynamic pressure. Table 1 summarizes data of this experiment pertinent to comparison with the present theory. Detailed velocity profiles were not obtained, instead, Dobson assumed a constant drag coefficient of .0012 based on the wind speed at 5 meters, U_5. From this, the u_* values shown were calculated.

The assumptions made in section 3 about the relative sizes of the length scales are all well-met in this experiment. The rms surface displacement greatly exceeds the viscous sublayer thickness (cf Table 1) and, with the exception of run 6, most of the contribution to σ comes from large amplitude, ungrowing waves. The amplitude of the fastest-growing waves is very small.

The runs may initially be divided into two groups based on the wind speed. Since the minimum phase speed for water waves is 23.4 cm/sec,

Run	U_5	u_*	σ	τ_w/τ	E_w	E	U_k	$\bar{c}_d$	U_k'	U_k'/U_k	k_s	$10\sigma/u_*$
1	220	7.6	4.15	1.6	13	8	150	370	260	1.73	11.7	.19
2a	320	11.0	4.35	1.6	43	27	220	570	395	1.79	12.2	.13
2b	310	10.7	3.5	1.1	29	26	205	345	275	1.34	9.8	.13
3	340	11.7	5.0	1.1	30	27	235	385	310	1.32	14.0	.12
4a	800	27.6	4.9	.7	155	220	555	415	485	.87	13.8	.05
4b	700	24.1	4.65	.6	230	380	485	415	450	.93	13.1	.06
6	570	19.6	2.3	.8	60	75	360	270	315	.88	6.5	.07

Table 1

in those runs for which the shear velocity exceeds this value, separation will surely occur. We expect then, the theory developed in the preceeding sections to be directly applicable to runs 4a and 4b. Run 6, made at a marginal wind speed, will be discussed separately. In runs 1, 2a, 2b, and 3, u_* based on U_5, is less than the minimum phase speed, and the theory is expected not to apply directly. Run 5 was made at such a low wind speed that no wave growth occurred at any of the measured frequencies. This null result is in agreement with the present theory.

Figure 19-25 show the growth rates, β/s versus frequency as measured by Dobson (1971). The error bars shown are those which result from the uncertainty in both the pressure correlations and the wind speed. The solid lines represent the predictions of the theory using the airflow parameters based on the wind speed at 5 meters. The dashed lines are the predictions when wave-driven mean motions are taken into account. This is discussed in detail later in this section. In all cases, we have used $\gamma = 7.8$. This is the $\langle u^2 \rangle$ value at the edge of the linear region for flow over a smooth wall and is in close agreement with the

value measured over water waves. See discussion in section 2.

In Figure19-25 a vertical arrow indicates the frequency at which $\beta = \alpha_c$. Since the mathematical theory developed in section 3 accounts only for first-order wave-turbulence interactions, it strictly applies only for small β. The occurance of $\beta = \alpha_c$ may be expected to indicate the frequency at which the next order correction becomes important. We can estimate, qualitatively, the effects of the next order correction by the following argument. The effectiveness of the critical layer is its ability to cause mean flow quantities to be asymmetrically distributed about the crest of the growing wave. These quantities, in turn, force the streamflow pattern to be shifted downwind, causing work to be done on the wave. In the next order, the critical layer itself is shifted. If the critical layer were to shift forward by a quarter of a wavelength, 90°, the mixing would produce no asymmetry with respect to the crest, while a shift of 45° would produce the maximum amount of asymmetry.

To the extent that α_c is unchanged by the critical layer, $\beta = \alpha_c$ indicates a 45° phase shift. Thus, we expect $\beta = \alpha_c$ to be

associated with the breakdown of the linear theory and the occurance of a wave growth rate maximum. In the discussion which follows, these very conditions are shown to occur.

high-wind velocities

We first discuss the high- wind cases: runs 4a and 4b. Table 1 shows that the rate of energy delivered to the water by pressure forces, $\dot{E}_w$, is far greater in these cases than in any other. When the total energy flux, $\dot{E}$, is estimated by $\dot{E}=(\tau/\tau_w)\dot{E}_w$, we see that the total energy transferred is an order of magnitude larger than in the low wind cases. When an equilibrium is reached between the airflow and the water, we might expect the energy transfer to take on a form based only on dimensional arguments. The only combination of U_5, ρ_a, and g which has the units of $\dot{E}$ is $\rho_a U_5^3$. The two are proportional, with the constant of proportionality to be determined. The dimensionless constant which must enter any pressure driven coupling is s, the ratio of air and water densities. We might expect then that

$$\dot{E} = s\rho_a U_5^3 , \qquad (154)$$

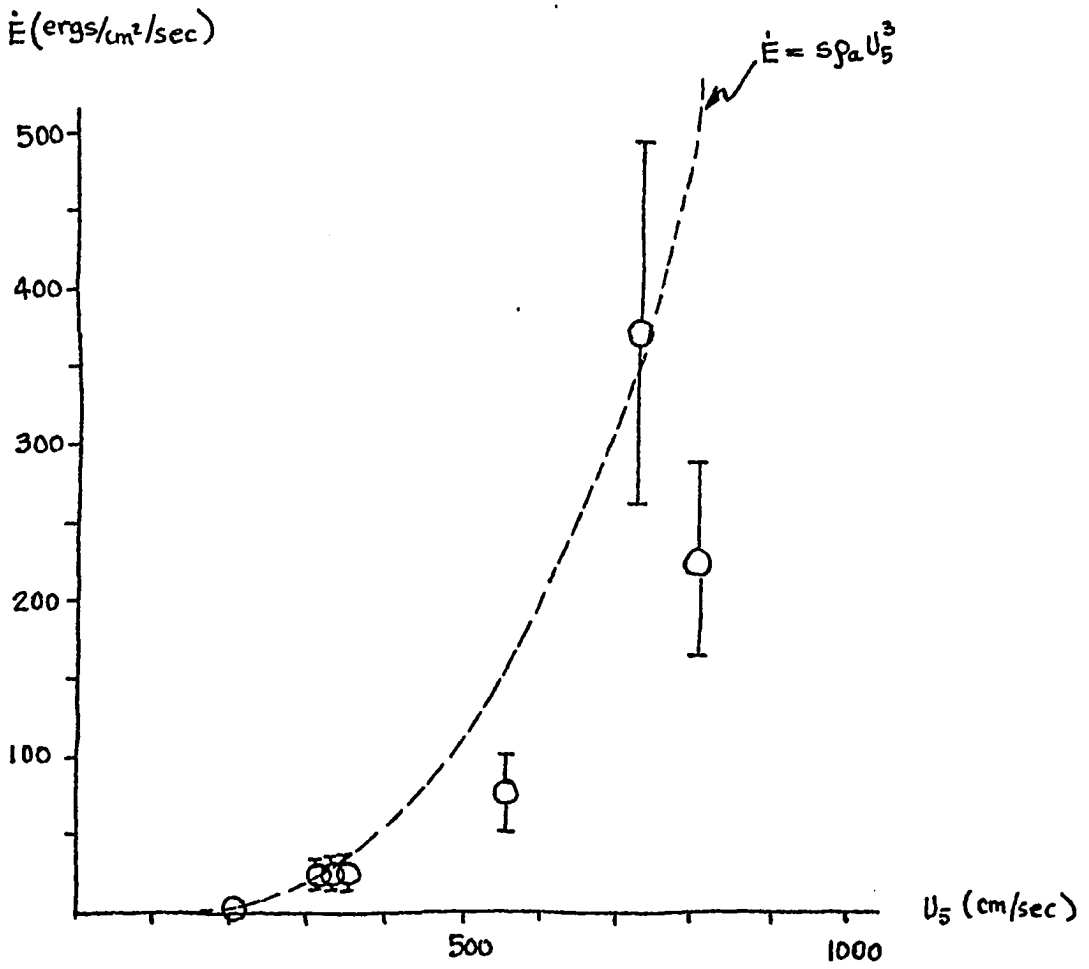

Figure 18. The total energy flux from the air to the water surface for each of Dobson's runs, plotted versus the wind speed at 5 meters above the mean water level. The dashed curve was derived from dimensionality arguments. The two runs which fall below the theoretical curve both represent cases in which equilibrium was not reached because of fetch or duration limitations.

holds under equilibrium conditions. Figure 18 shows that our choice has been fortunate, since the $\dot{E}$ values fall close to this curve. The two exceptions are runs 4a and 6, both of which represented duration limited or fetch limited conditions. In any event, the importance of the high wind cases to the total energy and momentum flux is clearly underscored.

We have already pointed out that the present theory should apply directly to the high-wind cases. Figures 19 and 20 show that the growth rates, hence the energy and momentum fluxes, are predicted within experimental error. The growth rates become non-zero at a fairly well-defined frequency, which is in close agreement with the predicted value, that is, the frequency at which the critical layer enters the linear region. This is another indirect confirmation of the thickness of the linear region. The $\beta = \alpha_c$ point corresponds to the measured growth rate maximum and to the limits of agreement with the present linear theory, as anticipated earlier. In short, at high wind velocities, the measurements are well-explained in every respect.

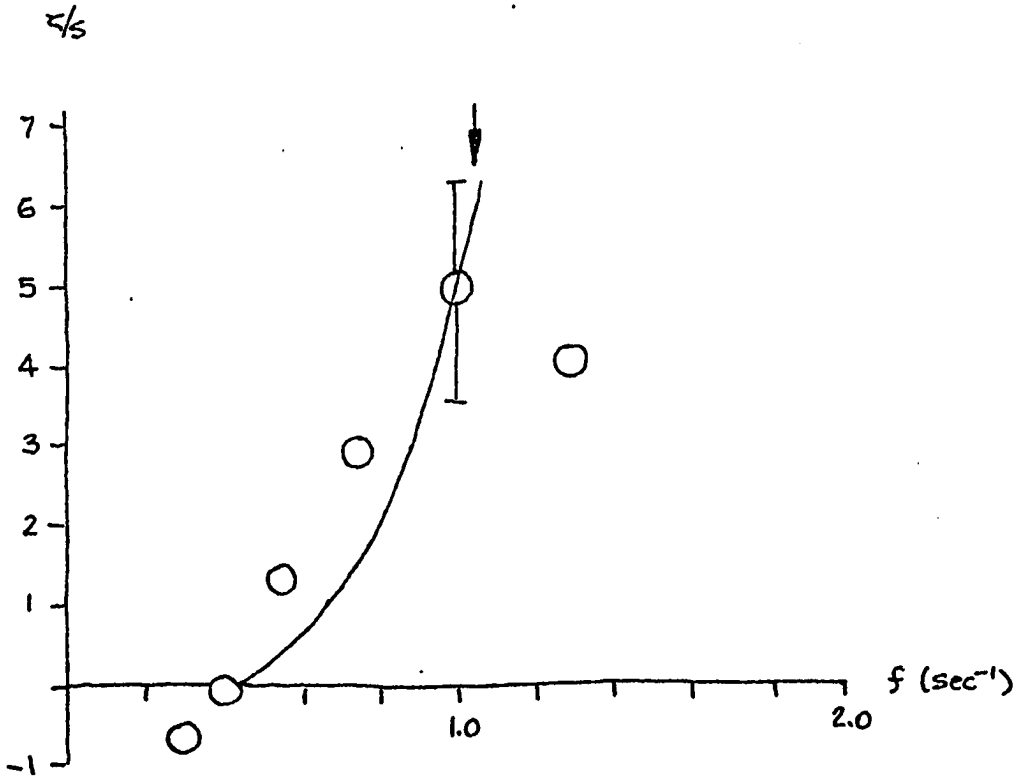

Figure 19. Comparison of the present theory with Dobson's run # 4a. Data taken at the highest wind speed, U_5=800, cgs. The dashed and solid curves coincide in this case.

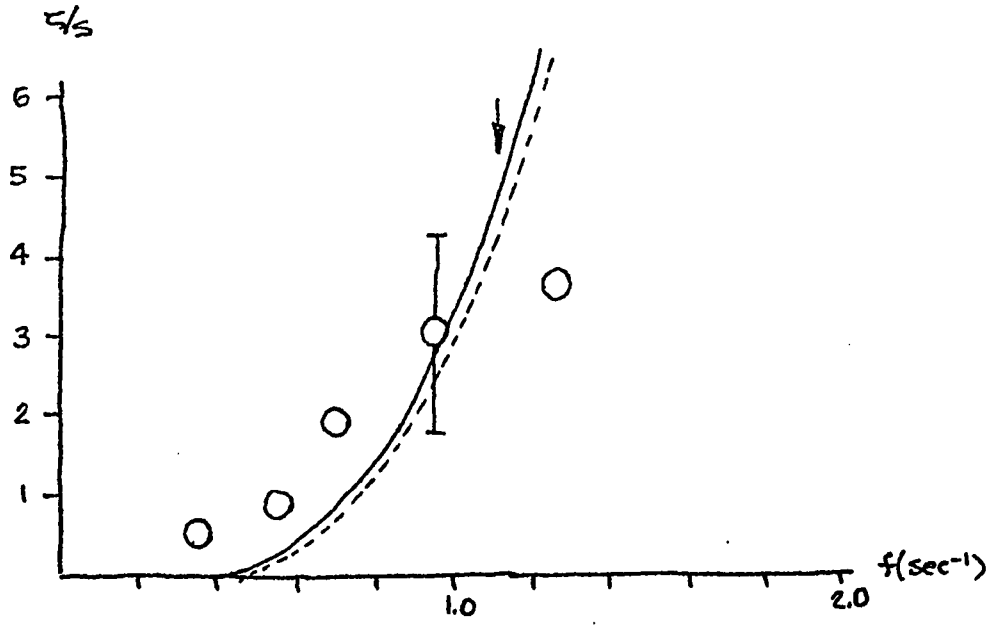

Figure 20. Dobson's run #4b compared with the predictions of the present theory. This run was made at the second largest wind speed of U_5= 700 cm sec^{-1}.

run 6

Run 6 was made at a very short fetch under conditions in which the airflow and wave spectrum were in rapid development (see the discussion in Dobson (1971)). Low frequency growth is highly erratic and the pressure phase shift had a frequency dependence totally unlike any other run. See Figure for a comparison. The run was made during a light rain which may have some effect on the results. Despite this, and the low u_* value, the predictions are qualitatively correct as to the range and magnitude of the growth, and indicate closely the position and magnitude of the growth rate maximum. It would seem that there is some additional low frequency process, possibly involved with the rapid spectral developement, present, in addition to the separation mechanism. Although this data has limited applicability to the present theory, it undoubtably has direct bearing on the questions of initial formation.

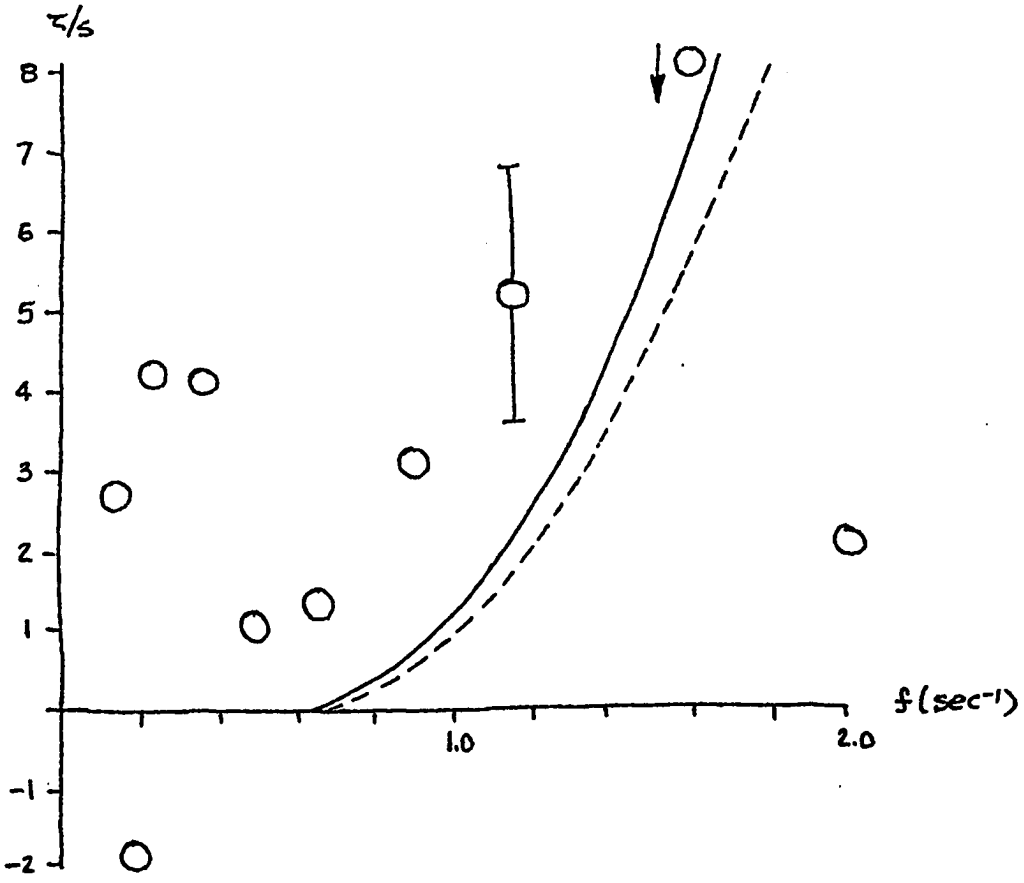

Figure 21. Comparison of the present theory with Dobson's run #6 made at U_5= 580 cm/sec.

low-wind velocities

At low-wind speeds, there is clearly disagreement between the predictions based on the wind characteristics at 5 meters, the solid lines, and the measurements. The source of this discrepancy is that the energy transfer depends on the square of the mean velocity supplying the energy. If the energy is supplied directly by the wind far above the surface, run 1, with a 5-meter wind speed of one quarter that of run 4a, would be expected to have a maximum growth rate of one-sixteenth that of run 4a. Instead, measurement shows the rate to be only a factor of two smaller! This emphasizes one of the most puzzeling aspects of wave generation: how do waves moving faster than the wind grow? The answer is that <u>they grow because of the mean air motions generated by other large amplitude waves</u>. The following discussion attempts to justify this claim. We note that we are concerned with the relatively short waves for which Longuet-Higgins mechanism is not applicable.

Inspection of the detailed distribution of surface waves (Dobson's Figure 9) reveals that the <u>dominant waves</u>, those waves which are at the

peaks of the power spectra, have phase velocities which are comparable to or greater than the wind velocities. Since these waves are very large, by their definition as peaks of the spectrum, they would be expected to cause non-linear effects in the airflow. We have already discussed in section 2 the non-linear effects of separation. Another effect is wave-driven mean motion. We might expect the air in the neighborhood of the surface to be pushed by the larger waves as well as by the wind far above the surface. Table 1 shows an average dominant wave speed, $\bar{c}_d$, obtained by averaging the phase speeds of the dominant waves of a given run, weighted by their heights in the spectral curve. (Data near the low-frequency peak in run 4a was not reported, so the same $\bar{c}_d$ as run 4b was used.) The true air velocity near the surface reflects both the influence of the wind, characterized by the U_k value calculated from U_5 measurements, and the influence of the large waves, characterized by $\bar{c}_d$. We shall use the average of U_k and $\bar{c}_d$, which we shall call U_k', as an estimate of the correct air velocity at the edge of the linear region. This guarantees that when the waves and wind move with the same speed, there

will be no correction to the motion.

The dashed curves in Figure 19-25 show that the predictions which result from using U_k' are quite close to the measured values. The frequency range over which growth occurs is reproduced and the $\beta = \alpha_c$ point correlates with the breakdown of the linear theory and with the growth rate maxima, although the maxima are not as distinct as in the high wind cases. The close agreement with each aspect of the measurements supports our contention of wave-driven mean motion.

There is additional support for this assumption. In those cases where $\bar{c}_d$ exceeds U_k, the use of U_k' increases the shear in the linear region and decreases the shear above. Thus, wave drag is increased at the expense of shear drag. In fact, the waves do work on the air, resulting in a negative shear drag and a wave drag which exceeds the total momentum flux! This is exactly the situation indicated by Dobson's data: when U_k' exceeds U_k, τ_w exceeds τ (as calculated from the drag coefficient). More precisely, the ratio (U_k'/U_k), which measures the increased wave drag due to the assumed wave-driven mean motions, is in almost perfect agreement with the measured

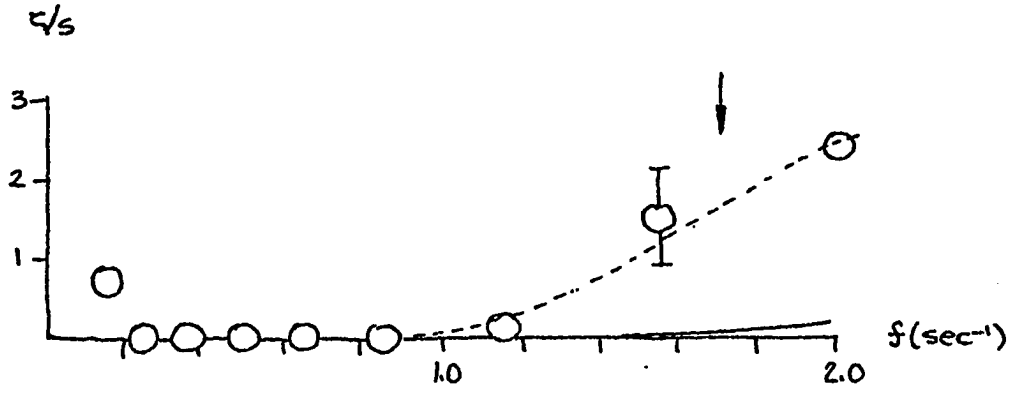

Figure 22. Comparison of the present theory with Dobson's run #1 made at the very low wind speed of 220 cm/sec. The influence of wave-driven mean motion is quite pronounced (the dashed line).

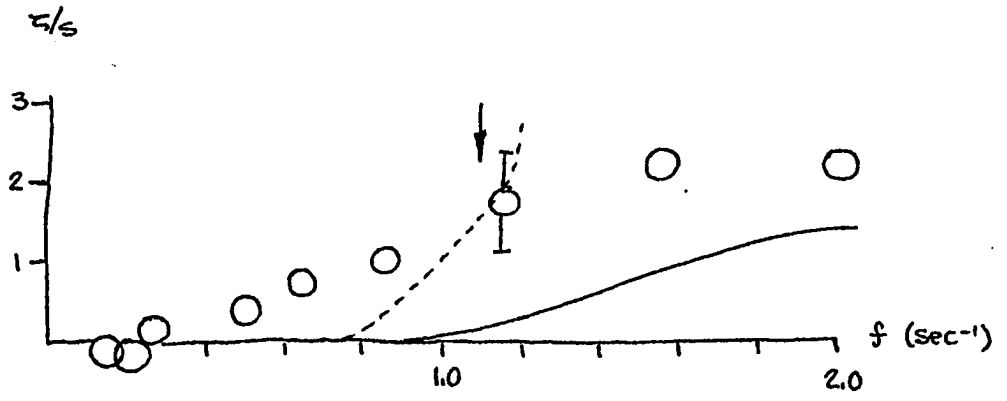

Figure 23. Comparison of the present theory with Dobson's run# 2a, made at the low wind speed of 320 cm/sec.

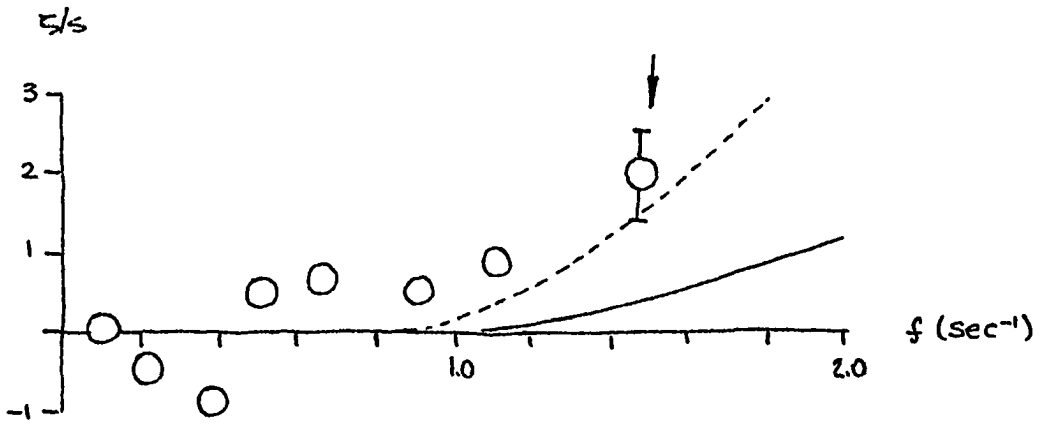

Figure 24. Comparison of the present theory with Dobson's run # 2b made at the low wind speed of 310 cm/sec.

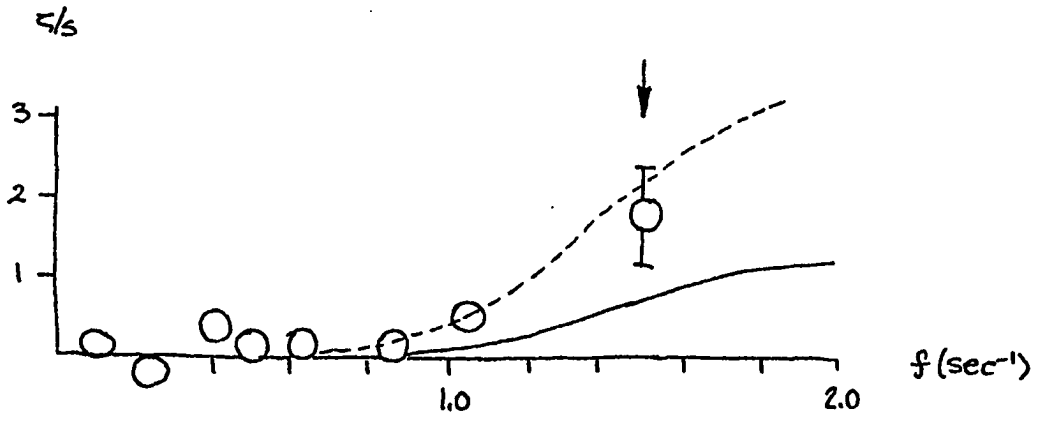

Figure 25. Comparison of the present theory with Dobson's run #3 made at the low wind velocity of 340 cm/sec.

values of (τ_w/τ). See Table 1 and Figure 26. Simiarly, at high wind speeds, when the waves slow down the wind driven motions, (τ_w/τ) is less than 1. In Figures 19-21, the correction of the high-wind predictions for these wave-retarding effects leads to no substantial change in the earlier agreement.

There is yet another experimental result which supports this hypothesis of wave -driven mean motion. At low wind velocities, when $\bar{c}_d$ exceeds U_k, not only is the shear changed but the velocity profile itself is altered. Figure 27 shows that the velocity profile will develop a kink near the water surface above the wave heights as the wave-driven corrections merge with the profile due to the wind. This very effect has been reported in sea measurements by Yefimov and Sizov (1969), Nan-niti, Fujiki, and Akamatsu (1968), Takeda (1963), and many others. Typical mean velocity curves found by the Russian authors are shown in Figure 27 for comparison. The similarity is unmistakable. Thus we find considerable experimental support for the concept of wave-driven mean motions, in addition to the explanation of wave growth at low wind speeds.

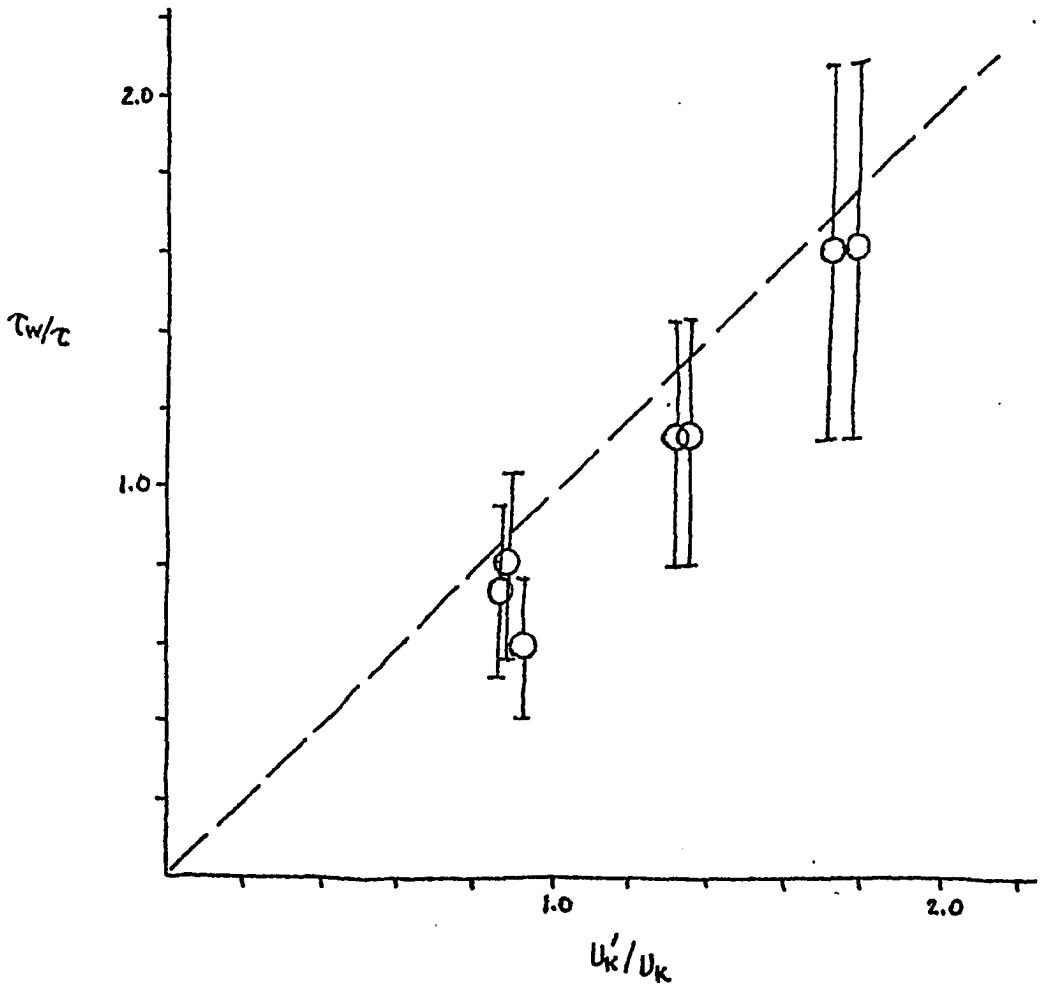

Figure 26. Comparison of the measured ratio of the momentum flux carried by pressure forces to the total flux (τ_w/τ) and the theoretical prediction based on the effects of wave-driven mean motions (U_K'/U_K). The dotted line is the expected relation if wave and wind contributions are equal.

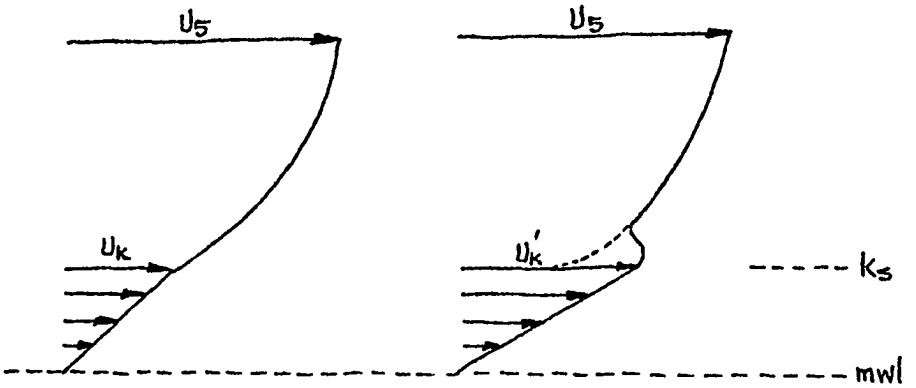

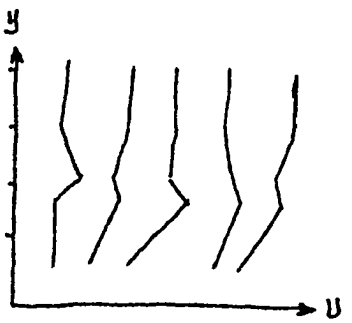

Yefimov and Sizov

Figure 27. Illustration that wave-driven mean motions can lead to "kinks" in the mean velocity profile as measured by many authors. The upper figure on the left shows the mean velocity profile if only the wind drives the air near the surface: a logarithmic profile joined to a linear one. The upper right figure shows, schematically, the effects of an increased velocity in the linear region due to wave-driven motion. The joining of the two effects leads to a "kink" in the measured profile somewhere above the average wave height. The lower figure is taken from a report by Yefimov and Sizov showing the experimentally measured kinks found over fast moving swell.

The details of wave-driven mean motion must be more carefully derived in a complete treatment of the air-water interaction. However, using the simple assumption of equal contributions from wind and waves, we have made a strong arguement for the basic mechanism at work at low wind speeds: energy is transferred to the growing waves through the action of the critical layer on the mean turbulent stress gradients. The energy in the mean shear is supplied in part by wave-driven motions of the large amplitude components.

One might ask: how did the large-amplitude waves come to be in the first place? Two possibilities suggest themselves. First, mechanisms other than pressure forces may be at work. A most attractive candidate is the "spray" mechanism of Longuet-Higgins. The wind causes breaking which drives the large waves, which in turn drives a mean motion which is tapped by the critical layer mechanism. A less interesting explanation is that the waves were generated at another place and an earlier time, and because of their large phase speeds, have overtaken the slower wind to produce the air-sea conditions observed

at the time of the measurements.

4.5 SUMMARY

In this section we developed a theory of ocean wave generation based on the instability of turbulent flows with stress gradients studied in the last section. The stress gradients in the oceanographic case result from airflow separation from the large waves. In comparisons with other theoretical work, it was shown that the theory was unique in that it takes into account the effects of sea conditions on the mean airflow and that it is a deductive result involving no free parameters. The predictions of the theory are in detailed agreement with the field measurements of Dobson. The frequency range over which growth occurs and the magnitude of the growth rates are reproduced and the limits of the linear theory and the position of the growth rate maximum follow directly from the physical model of the critical layer. At low-wind velocities, the importance of wave-driven mean motions is demonstrated by explaining the detailed features of growth rates, the fraction of the momentum flux carried by wave drag, and "kinks" in the mean velocity profile

reported by many authors. By including wave-driven effects, the energy and momentum transfer to the sea is well-explained under all wind conditions.

BIBLIOGRAPHY

Abramowitz M. and Segun I.A. 1965 Handbook of Mathematical Functions. Dover.

Arie M. and Rouse H. 1956 J. Fluid Mech. 1, 129.

Baines W.D. and Knapp D.J. 1965 Wind driven water currents. Proc. ASCE hy2, 205.

Batchelor G.K. 1953 The Theory of Homogeneous Turbulence. Cambridge Univ. Press.

Benjamin T.B. 1959 Shearing flow over a wavy wall. J. Fluid Mech. 6, 161.

Benjamin T.B. 1960 Effects of a flexible boundary on hydrodynamic stability. J. Fluid Mech. 9, 513.

Bole J.B. and Hsu E.Y. 1966 Response of gravity water waves to wind excitation. J. Fluid Mech. 25, 657.

Bradshaw P. 1966 The effects of initial conditions on the development of a free shear layer. J. Fluid Mech. 26, 225.

Bryant P.J. 1966 Wind generated water waves. PhD dissertation, University of Cambridge.

Chang P.C., Plate E.J., and Hidy G.M. 1971 Turbulent air flow over the dominant component of wind-generated water waves. J. Fluid Mech. 47, 183.

Charnock H. 1955 Wind stress on a water surface. Quart. J. R. Met. Soc. 81, 639.

Coles D. 1956 Law of the wake in the turbulent boundary layer. J. Fluid Mech. 1, 191.

Conte S.D. and Miles J.W. 1959 On the numerical integration of the Orr-Sommerfeld equation. J. SIAM 7, 361.

Corrisin S. and Kistler A.L. 1954 NACA TN 3133.

Craik A.D. 1968 Resonant gravity-wave interactions in a shear flow. J. Fluid Mech. 34, 531.

Crow S. 1968a Turbulent Rayleigh shear flow. J. Fluid Mech. 32, 113.

Crow S. 1968b Viscoelastic properties of fine-grained incompressible turbulence. J. Fluid Mech 33, 1.

Danner W.P. 1966 A mixing length treatment of the effects of turbulence on the wind generation of water waves. M. Sc. dissertation, U.S. Naval Postgraduate School, Monterey.

Davis R.E. 1969 On the high Reynolds number flow over a way boundary. J. Fluid Mechl 36, 337.

Davis R.E. 1970 On the turbulent flow over a wavy boundary. J. Fluid Mech. 42, 721.

Davis R.E. 1972 On the prediction of turbulent flow over a wavy boundary. J. Fluid Mech. 52, 287.

Davis R.E. 1973 Perturbed turbulent flow, eddy viscosity and the generation of turbulent stresses. (in preparation).

Davis S.H. 1970 Finite amplitude instability of time-dependent flows. J. Fluid Mech. 45, 33.

Dobson F.W. 1971 Measurements of atmospheric pressure on wind generated sea waves. J. Fluid Mech. 48, 91.

Drazin P.G. 1970 Kelvin-Helmholtz instability of finite amplitude. J. Fluid Mech. 42, 321.

Eckart, C. 1953 The generation of wind waves on a water surface. J. Appl. Phys. 24, 1485.

Esch R.E. 1957 The instability of a shear layer between parallel streams. J. Fluid Mech. 3, 289.

Feldman S. 1957 On the hydrodynamical stability of two viscous incompressible fluids in parallel shearing motion. J. Fluid Mech. 3, 343.

Gaster M. 1962 A note on the relation between temporally-increasing and spatially-increasing disturbances in hydrodynamic stability. J. Fluid Mech. 15, 222.

Glauert M.B. 1960 The method of images in shear flow. J. Fluid Mech. 9, 561.

Gradshteyn I.S. and Ryzhik I.M. 1965 Tables of Integrals, Series, and Products. Academic Press.

Grosch C.E. and Salwen H. 1968 The stability of steady and time-dependent plane Poiseuille flow. J. Fluid Mech. 34, 177.

Gupta A.K., Landahl M.T., and Mollo-Christensen E.L. Experimental and theoretical investigation of the stability of air flow over a water surface. J. Fluid Mech. 33, 673.

Haberman R. 1972 Critical layers in parallel flows. Stud. Appl. Math. 51, 139.

Hamada T. 1968 On some properties of wind over water waves. Rep. Port and Harb. Res. Inst. 7, 4.

Hasselmann K. 1971 On the mass and momentum transfer between short gravity waves and larger-scale motions. J. Fluid Mech. 50, 189.

Helmholtz H 1868 Uber discontinuirlishe Flussigkeitsbewegungen. Mber. preuss. Akad. Wiss., 215.

Hidy G.M. and Plate E.J. 1965 Frequency spectrum of wind-generated waves. Phys Fluids 8, 1387.

Hidy G.M. and Plate E.J. 1966 Wind action on water standing in a laboratory channel. J. Fluid Mech. 26, 651.

Hildebrand F.B. 1962 Advanced Calculus for Applications. Prentice-Hall.

Hinze J.O. 1959 Turbulence. McGraw-Hill.

Holstein H. 1950 Uber die ausser und innere Riebungsschicht bei Storungen laminaren Stromungen. Z. angew Math. Mech. 30, 25.

Hughes B.A. and Stewart R.W. 1961 Interaction between gravity waves and a shear flow. J. Fluid Mech. 10, 385.

Hussain A.K.M.F. and Reynolds W.C. 1970 The mechanics of an organized wave in turbulent shear flow. J. Fluid Mech. 41, 241.

Jeffreys H. 1925 On the formation of water waves by wind. Proc. Roy. Soc. A 107, 189.

Jeffreys H. 1926 On the formation of water waves by wind (second paper). Proc. Roy. Soc. A 110, 241.

Joseph D.D. 1969 Eigenvalue bounds for the Orr-Sommerfeld equation. Part 2. J. Fluid Mech. 36, 721.

Kelvin Lord 1871 Influence of wind and capilarity on waves in water assumed frictionless. Mathematical and Physical Papers, volume IV.

Kendall, J.M. 1970 The turbulent boundary layer over a wall with progressive surface waves. J. Fluid Mech. 41, 259.

Kinsman B. 1962 Wind Waves. Prentice-Hall.

Klebanoff P.S. 1954 NACA TN 3178.

Kline S.J., Reynolds W.C., Schraub F.A., Runstadler P.W. 1967 The structure of turbulent boundary layers. J. Fluid Mech. 30, 741.

Kogelman S. and DiPrima R.C. 1970 Stability of spatially periodic supercritical flows in hydrodynamics. Phys. Fluids 13, 1.

Kondo J., Fujinawa Y., and Naito G. Wave-induced wind fluctuations over the sea. J. Fluid Mech. 52, 751.

Lamb Sir H. 1932 Hydrodynamics. Cambridge Univ. Press.

Landau L.D. and Lifshitz E.M. 1959 Fluid Mechanics. Addison-Wesley.

Laufer J. 1954 NACA Tech. Rep. 1174.

Lighthill M.J. 1962 Physical interpretation of the mathematical theory of wave generation by wind. J. Fluid Mech. 14, 385.

Lin C.C. 1955 The Theory of Hydrodynamic Stability. Cambridge Univ. Press.

Lin S.P. 1969 Finite amplitude stability of a parallel flow with a free surface. J. Fluid Mech. 36, 113.

Long R. 1971 PhD dissertation, University of Miami.

Longuet-Higgins M.S. 1962 The directional spectrum of ocean waves and processes of wave generation. Proc. Roy. Soc. A 265, 286.

Longuet-Higgins M.S. 1969a A nonlinear mechanism for the generation of sea waves. Proc. Roy. Soc. A 311, 371.

Longuet-Higgins M.S. 1969b Action of a variable stress at the surface of water waves. Phys. Fluids 12, 737.

Longuet-Higgins M.S. 1973 A model of flow separation at a free surface. J. Fluid Mech. 57, 129.

Lyne W.H. 1971 Unsteady viscous flow over a wavy wall. J. Fluid Mech. 50, 33.

Malkus W.V.R. 1957 Outline of a theory of turbulent shear flow. J. Fluid Mech. 2, 521.

Manton M.J. 1972 On the generation of sea waves by a turbulent wind. Boundary-Layer Meteor. 2, 348.

Miles J.W. 1957 On the generation of surface waves by shear flows. J. Fluid Mech. 3, 185.

Miles J.W. 1958 On the disturbed motion of a plane vortex sheet. J. Fluid Mech. 4, 539.

Miles J.W. 1959 On the generation of surface waves by shear flows. Part 2. J. Fluid Mech. 6, 568.

Miles J.W. 1960a On the generation of surface waves by shear flows. Part 3. J. Fluid Mech. 6, 583.

Miles J.W. 1960b On the generation of surface waves by turbulent shear flows. J. Fluid Mech. 8, 469.

Miles J.W. 1962a A note on the inviscid Orr-Sommerfeld equation. J. Fluid Mech. 13, 427.

Miles J.W. 1962b On the generation of surface waves by shear flows. Part 4. J. Fluid Mech. 13, 433.

Miles J.W. 1967 On the generation of surface waves by shear flows. Part 5. J. Fluid Mech. 30, 163.

Mills R.D. 1968 Numerical and experimental investigation of the shear layer between two parallel streams. J. Fluid Mech. 33, 591.

Motzfeld H. 1937 Die turbulente stromung an welligen wanden. Z. ang. Math. Mech. 17, 193.

Nan-niti T., Fujiki A., and Akamatsu H. 1968 Micro-meteorological observations over the sea. J. Oceanog. Soc. Japan 24, 281.

Neumann G. 1952 On wind generated ocean waves. NYU Department of Meteorology Technical Report.

Phillips O.M. 1957 On the generation of waves by a turbulent wind. J. Fluid Mech. 2, 417.

Phillips O.M. 1958 The equilibrium range in the spectrum of wave-generated waves. J. Fluid Mech. 3, 426.

Phillips O.M. 1960a The low frequency components of the spectrum of wind-generated waves. J. Mar. Res. 19, 57.

Phillips O.M. 1960b On the dynamics of unsteady gravity waves of finite amplitude. J. Fluid Mech. 9, 193.

Phillips O.M. 1966 The Dynamics of the Upper Ocean. Cambridge Univ. Press.

Phythian R. 1972 Some variational methods in the theory of turbulent diffusion. J. Fluid Mech. 53, 469.

Pierson W.J. 1952 A unified mathematical theory for the analysis, propagation and refraction of storm generated ocean waves. NYU Tech. Rep.

Pierson W.J. and Neumann G. 1961 in Ocean Wave Spectra. Prentice-Hall.

Plate E.J. and Hidy G.M. 1967 Laboratory study of air flowing over a smooth surface onto small water waves. J. Geophys. Res. 72, 4627.

Plate E.J., Chang P.C., and Hidy G.M. 1969 Experiments on the generation of small waves by wind. J. Fluid Mech. 35, 625.

Sandborn V.A. and Liu C.Y. 1968 On turbulent boundary layer separation. J. Fluid Mech. 32, 293.

Schlichting H. 1959 Boundary Layer Theory. McGraw-Hill.

Schooley A.H. 1971 Diffusion sublayer thickness over wind-disturbed water surfaces. J. Phys. Oceanog. 1, 221.

Schubauer G.B. 1954 J. Appl. Phys. 25, 188.

Shemdin O.H. and Hsu E.Y. 1967 Direct measurement of aerodynamic pressure above a simple progressive gravity wave. J. Fluid Mech. 30, 403.

Snyder R.L. and Cox C.S. 1966 A field study of the wind generation of ocean waves. J. Mar. Res. 34, 141.

Stanton T., Marshall D., and Houghton R. 1932 The growth of waves on water due to the action of the wind. Proc Roy. Soc. A 221, 283.

Stewart R.H. 1970 Laboratory studies of the velocity field over deep-water waves. J. Fluid Mech. 42, 733.

Stewart R.W. 1971 The wave drag of wind over water. J. Fluid Mech. 10, 189.

Stuart J.T. 1958 On the non-linear mechanisms of hydrodynamic stability. J. Fluid Mech. 4, 1.

Stuart J.T. 1960 On the non-linear mechanisms of wave disturbances in stable and unstable parallel flows. J. Fluid Mech. 9, 353.

Sutherland A.J. 1968 Growth of spectral components in a wind-generated wave train. J. Fluid Mech. 33, 545.

Sverdrup H.U. and Munk W. 1947 Wind, sea and swell. Publ. Hydrog. Off. 601.

Takeda A. 1963 Wind profiles over sea waves. J. Oceanog. Soc. Japan. 19, 16.

Tam K.K. 1968 On the asymptotic solution of the Orr-Sommerfeld equation by the method of multiple scales. J. Fluid Mech. 34, 145.

Tollmein W. 1929 The production of turbulence. NACA Tech. Memo 609.

Townsend A.A. 1956 The structure of Turbulent shear flow. Cambridge Univ. Press.

Townsend A.A. 1972 Flow in a deep turbulent boundary layer over a surface distorted by water waves. J. Fluid Mech. 55, 719.

Ursell F. 1956 Wave generation by wind. in Surveys in Mechanics. Cambridge University Press.

Van Atta C.W. and Chen W.Y. 1970 Structure functions of turbulence in the atmospheric boundary layer over the ocean. J. Fluid Mech. 44, 145.

Wallace J.M., Eckelmann H., and Brodkey R.S. 1972 The wall region in turbulent shear flow. J. Fluid Mech. 54, 39.

Watson J. 1960 On the non-linear mechanisms of wave disturbances in stable and unstable parallel flows. J. Fluid Mech. 9, 371.

Wiegel R.L. and Cross R.H. 1966 Generation of wind waves. Proc ASCE WW2, 1.

Willmarth W.W. and Lu S.S. 1972 Structure of the Reynolds stress near the wall. J. Fluid Mech. 55, 65.

Willmarth W.W. and Wooldridge C.E. 1962 Measurements of the fluctuating pressure at the wall beneath a thick turbulent boundary layer. J. Fluid Mech. 14, 187.

Wu J. 1968 Laboratory studies of wind-wave interactions. J. Fluid Mech. 34, 91.

Wu J. 1970 Wind-wave interactions. Phys. Fluids 13, 1926.

Yefimov V.V. and Sizov A.A. 1969 Experimental study of the field of wind velocity over waves. Izv. Atmos. and Oceanic Phys. 5, 930.

Yih C.S. 1968 Fluid Mechanics. McGraw-Hill.

Zaugustin K., Hsu E.Y., Street R.L., and Perry B. 1966 Flow over a moving boundary in relation to wind generated waves. Dept. Civil Eng. Tech. Rep. 60. Stanford University.

APPENDIX

The formulae of section 4.1 were implemented by a FORTRAN computer program, written and executed on the University of Cincinnati's IBM 360/70 time-sharing facilities. The coding of the program is shown on the next page.

```
LIST

JHSP          20:12    2/6/73 SWORCC CALL/OS

100 DIMENSION F(12),BETA(12),ZETA(12),FC(12),PHI(12)
110 PI=4.*ATAN(1.)
120 32 READ(5,*)ON
130 UU=7.8
140 7 WRITE(6,10)
150 10 FORMAT(' U5,UK,TAUW,SIGMA')
160 READ(5,*)U5,UK,TAUW,SIG
170 IF(U5.EQ.0) GO TO 32
180 XKS=2.82*SIG
190 DO 2 NFC=1,11
200 FC(NFC)=.2+(NFC-1)*.2
210 C=490./PI/FC(NFC)
220 XK=2.*PI*FC(NFC)/C
230 U1=(U5-UK)/ALOG(500./XKS)
240 USTAR=U5/29.
250 A=UK/XK/XKS/C
260 B=UK/C-1.
265 AB=B/A
270 IF(C.GT.UK)GO TO 13
280 F1=EXP(-1./A)*A**2*(2.-EXP(-AB)*(2+2*AB+AB**2))
290 F2=(PI*U1/C)**2/6.+((.5772157+ALOG(XK*XKS))*(U1/C)-B)**2
300 N=1
310 F3=0.
320 TERM=-XK*XKS
330 4 Y=B**2-2*B*U1/C/N+2*(U1/C/N)**2
340 F3=F3+TERM*Y
350 IF(ABS(TERM*Y).LT..001) GO TO 3
360 N=N+1
370 TERM=-TERM*XK*XKS/N
380 GO TO 4
390 13 F1=0.
400 F2=0.
410 F3=0.
420 3 F(NFC)=F1+F2+F3
430 CC=(XK*XKS*USTAR/UK)**(2./3.)
440 ZETA(NFC)=PI*980*XKS*(F(NFC)/UK)**2*(TAUW+.74*UU*CC)
450 2 CONTINUE
460 IF(ON.EQ.1) GO TO 31
470 WRITE(6,11)(FC(I),I=1,11)
480 11 FORMAT(' FREQ. =',11(1X,F4.1))
490 WRITE(6,5)(F(I),I=1,11)
500 5 FORMAT(' ALPHA =',11(1X,F4.1))
510 31 CONTINUE
520 WRITE(6,8)(ZETA(I),I=1,11)
530 8 FORMAT(' ZETA/S=',11(1X,F4.1))
540 GO TO 7
550 END
```